Evapotranspiration over an Agricultural Region Using a Surface Flux/Temperature Model Based on NOAA-AVHRR Data

O. TACONET, R. BERNARD AND D. VIDAL-MADJAR

CNET/CNRS/CRPE, 92131 Issy-les-Moulineaux, France

(Manuscript received 11 August 1984, in final form 18 August 1985)

ABSTRACT

The possibility of using infrared surface temperatures from satellites (NOAA, GOES) for inferring daily evaporation and soil moisture distribution over large areas (10^2 to 10^5 km^2) has been extensively studied during the past few years. The methods are based upon analysis of the surface energy budget, but treating surface transfers as over bare soils. In this context, we have developed a methodology using infrared surface data (from NOAA-7) as input data, in a one-dimensional boundary layer/vegetation/soil model, including a parameterization of transfers within the canopy, based on the formalism of Deardorff which allows the use of a small number of mesoscale surface vegetation parameters.

As shown from the model sensitivity tests, a single surface temperature measured near midday (provided by NOAA-7) is sufficient for obtaining the surface energy fluxes over dense vegetation and for deriving the only governing parameter that remains, the bulk canopy resistance to evaporation, a different concept from moisture availability used for bare soils. The objective of the model in predicting the area-averaged surface fluxes and canopy resistances over dense vegetation is analyzed in conjunction with experimental surface flux measurements for three cases with cloudless NOAA images over a flat monocultural region (the Beauce in France). In the absence of a current capability for routine daily soil moisture observation over an agricultural region, an area-averaged evaluation of the soil moisture can be derived from the canopy resistance obtained by this methodology, using an empirical expression relating this resistance to the root zone water content. Spatial gradient of water content between two areas of Beauce with different soil drainage properties is thus evaluated.

1. Introduction

The knowledge of surface energy fluxes, soil moisture and substrate thermal inertia can provide insight into the state of the soil and its vegetation cover. Therefore, the demand for evapotranspiration and soil moisture information over large areas (10^2 to 10^5 km^2) is increasing in a variety of scientific fields, including hydrology, agriculture and weather prediction.

The possibility of using infrared (IR) surface temperature measurements from satellites in order to derive these surface and substrate quantities has been extensively studied during the past few years. Although the methods for using satellite-derived surface temperatures are based upon analysis of the energy budget of the earth's surface, these methods may be divided into two classes.

In the first, which we refer to as semi-empirical and statistical, the methods employ an approximate solution of the budget equation leading to semi-empirical formula relating evapotranspiration and moisture to the surface temperature (Idso et al., 1977; Seguin and Itier, 1983).

In the second class, analytical and numerical methods are based upon the solution of the inverse problem for both heat and mass transfers. Thus Watson (1975), Price (1977) and recently Becker et al. (1982) have shown the interest of Fourier models to extract thermal inertia from the diurnal temperature range, and, to determine surface moisture availability. The same basic physical principles have been used in subsequent numerical models in which the magnitude of the diurnal temperature range is related both to thermal inertia and moisture availability (Carlson and Boland, 1978; Carlson et al., 1981).

None of the methods presented above explicitly treat the vegetation, referring only to physical mechanisms above bare soil. The role of vegetation has been considered by Wetzel and Atlas (1983) who applied a very simplified parameterization in a one-dimensional boundary layer/vegetation/ground model, using satellite temperatures over a large heterogeneous region (GOES image with 10 km of resolution). The method chosen to include the vegetation is to overlay the ground model, comprising several layers, by an additional layer, called the vegetation layer, where the thermal flux through it is computed, given its mass equal to the biomass, and its specific heat capacity equal to that of liquid water, since much of the mass of vegetation is simply water. The radiative surface temperature is, therefore, the temperature of this "vegetation" layer. The concept of moisture availability over the

surface in order to limit the evaporation rate is retained, but it is interpreted in terms of soil water content in the root zone and evaporative demand, based on observational studies (Wetzel and Atlas, 1983).

In the present study, the vegetation cover is taken into consideration by using a detailed model of the mechanisms at the interface atmosphere/vegetation/ground, based on the formalism of Deardorff (1978), an efficient one-layer foliage parameterization where bare ground and foliage coexist side by side. Deardorff model used a limited number of parameters in his formalism, which are only expected to be significant at the mesoscale, which will match the AVHRR scale (1 km resolution) here. The general idea for determining heat fluxes and soil canopy temperatures is to solve simultaneously the energy budget equations at ground level and at the canopy level by assuming an adequate partitioning of the available fluxes between vegetation and bare soil, whose relative amounts are related to the foliage density, the distinct resistances to evaporation of soil and foliage, and other considerations.

Despite the many simplifying assumptions in the Deardorff model, the parameters employed are numerous and exceed reasonable practical definition, at least solely with the aid of satellite imagery and meteorological observations. To simplify the problem of defining soil/vegetation parameters, we propose, as a first step, a study of the case of dense vegetation, where we can show that the number of parameters are reducible to four essential ones: for vegetation, its height, density (leaf area index LAI) and plant resistance to transpiration; and for soil, its mean water content in the root zone.

With the aid of sensitivity tests on these parameters, we will show that the single IR surface temperature measured near midday (1300 UT for the satellite NOAA-7) is sufficient in a region with a dense homogeneous canopy to infer the surface fluxes and, by inversion, the single dominant vegetation parameter. The midday surface temperature is then sensitive only to the mean stomatal resistance of the canopy; even the regional LAI is not needed accurately.

Therefore, in a first application, using radiometric temperature measurements at midday, for agricultural regions with dense canopy, the inversion of the interface model yields the surface fluxes and the mean resistance of the canopy, a very different concept from that of surface moisture availability used for bare soil, as the vegetation is a layer of negligible heat capacity. However, it should be added that, with no daytime heat storage in the foliage layer, the nighttime temperature (near 0300 UT with NOAA-7) over dense canopy does not hold further information on the different foliage variables. Moreover, from analysis of NOAA IR data over French flat agricultural regions, namely, Crau (Seguin et al., 1982) and Beauce (Cheevasuvit et al., 1984), it appears clearly that the surface temperature has a much greater variability and spatially coherent distribution during daytime (near 1300 UT with NOAA-7) and that the spatial gradients at night are very weak.

In a second step, by specifying from agronomical studies, the range and dependence of stomatal resistance upon water content in the root zone, seasonal physiology and type of vegetation (the most important factors involved), we can relate the derived mean stomatal resistance to available water in the root zone, without knowing precisely LAI, for dense canopies.

Therefore, after a description of the model formalization in section 2, we study in section 3 the influence, on the evapotranspiration and on the maximum surface temperature, of four important variables of soil and canopy, in the range suggested by previous agronomical studies over cereal covers.

In the last part of this paper (sections 4 and 5), on three days (5 May 1982, 11 July 1982 and 11 July 1983), we study the determination of the adapted sets of mesoscale surface variables to restore the NOAA IR temperature magnitude and spatial gradients over two flat agricultural subzones of Beauce, France, with dense homogeneous canopies. This allows a quantitative evaluation of the surface fluxes and plant resistance to transpiration, over the two zones, from which one can also infer the spatial distribution of water content.

Finally, a validation is proposed by comparison of the simulated fluxes with measurements of surface fluxes (net radiation and sensible heat flux) at two sites located in the two different representative subzones during the same periods. It shows that the radiometric satellite surface temperature, computed by the interface model, is sufficiently sensitive for simulating the correct surface fluxes, with the aid of a boundary layer model, when the aforementioned simplifications are incorporated in the vegetation parameters.

2. Theoretical model: Vegetation surface layer and planetary boundary layer

The methodology developed here uses the diurnal variation of NOAA IR temperature as an input in a model representing the mechanism controlling its evolution, i.e., feedback between the surface fluxes and the boundary layer growth and regulation of energy transfers by the ground and the vegetation.

The observed satellite-IR temperature represents a spatially averaged value (over a few square kilometers) of the radiative skin temperature over a composite scene that includes bare soil and various canopies. The complex mixing of surface elements cannot be expressed in a deterministic sense in a model, but instead must be parameterized in a simplified manner, similar to that of Deardorff (1978). Therefore, using his formalism, we choose to employ a limited number of parameters, which are only expected to be significant at the scale of the satellite resolution (a few square kilometers). It has been shown (Cheevasuvit et al., 1985),

using a picture segmentation procedure on the NOAA IR images at midday, that over the studied agricultural region, the Beauce Plateau, the spatial variability of temperature has a well defined signature. The region is divided into three or more large areas (greater than 20×20 km^2) of distinct mean surface temperature, within which the variability of temperature is very weak (around 1°–2°C). Hence, the surface parameters defined by the model are significant on the scale of these homogeneous subzones, which match also the grid size of the atmosphere predictive models. This allows the development of a coupled one-dimensional boundary layer/vegetation/ground model.

The surface layer model consists of a 1 m deep ground layer, a single thin vegetation layer ventilated by a surface turbulent layer (10 m deep). The atmospheric forcing at the top of the surface layer is not specified, but predicted from an atmosphere boundary layer model (2500 m high), allowing the model to be used in areas where no continuous meteorological data are available. Since we consider stable anticyclonic conditions, we can ignore to some extent the problem of mesoscale advection. Thus, the boundary layer model need only be one dimensional. We choose a so-called KE model (Therry and Lacarrère, 1983), with a rather simple closure scheme, in which the eddy exchange coefficients are related to the eddy kinetic energy. An overview of the coupled model "canopy surface layer/boundary layer" is presented in Fig. 1.

We now discuss in more detail the surface model, which has been derived from Deardorff (1978), but which has not been described elsewhere in the literature.

a. Surface model

From Deardorff (1978), the general idea for determining heat fluxes and soil–canopy temperatures is to solve simultaneously the energy budget equations at the ground level and at the canopy level. Thus, the partition of the energy and momentum fluxes between the ground and the canopy has to be parameterized.

1) RADIATION PARTITION

As in Deardorff (1978), the vegetation is assumed to be a single foliage layer, with negligible heat capacity, shielding more or less completely the ground.

The key parameter for the radiation partition is the average shielding factor σ_f, defined by Deardorff as the

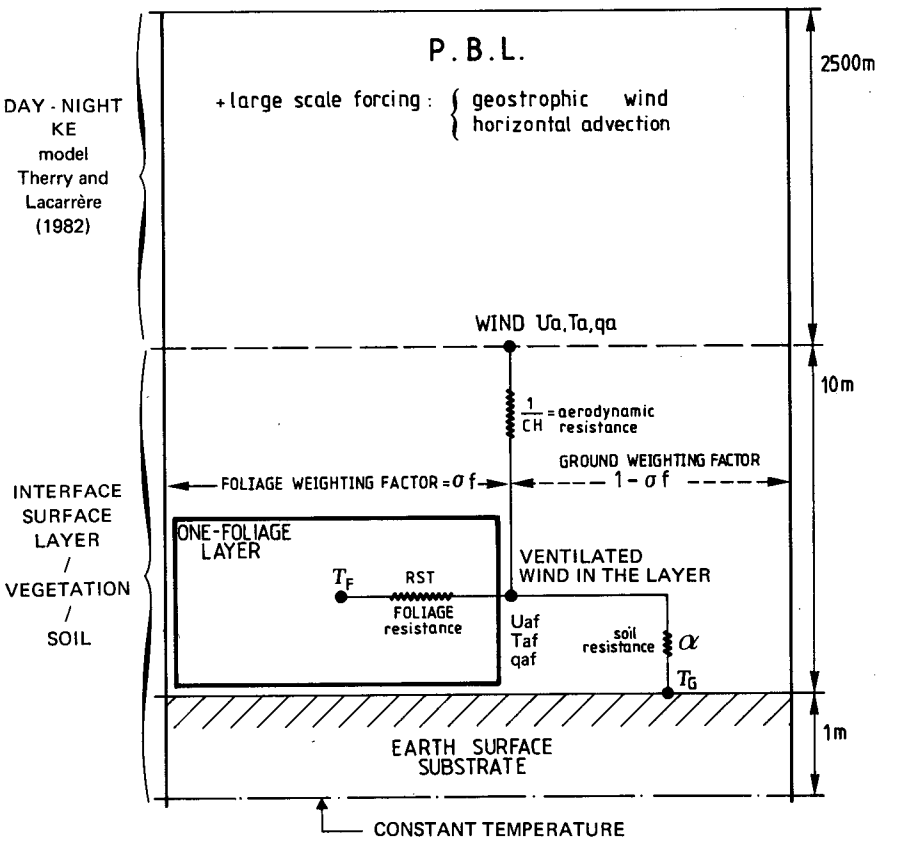

FIG. 1. Basic framework of model.

extent that foliage prevents shortwave and longwave radiation from reaching the ground. The partition, in Deardorff, is obtained by a linear interpolation with σ_f between radiation above bare soil and that applicable with a dense canopy. Here, a slightly different approach is to consider the radiation balance for a two layer system. The lower layer is the ground of albedo α_{sg}. The upper layer, the canopy, is assumed to be a semitransparent layer characterized by a reflectivity of $\sigma_f\alpha_{sf}$, an absorptivity of $(1 - \alpha_{sf})\sigma_f$ and a transmissivity of $(1 - \sigma_f)$, where α_{sf} is the foliage albedo. It allows internal reflection trapped between soil and canopy to be nonnegligible when the albedos are different from 1.

Thus, we obtain, for available visible radiation at ground level,

$$R_{sg} = S^{\downarrow}\frac{(1 - \sigma_f)(1 - \alpha_{sg})}{1 - \sigma_f\alpha_{sg}\alpha_{sf}}, \quad (1)$$

for the canopy,

$$R_{sf} = S^{\downarrow}(1 - \alpha_{sf})\sigma_f\left[1 + \alpha_{sg}\frac{(1 - \sigma_f)}{1 - \sigma_f\alpha_{sg}\alpha_{sf}}\right] \quad (2)$$

where $S^{\downarrow}$ is incoming shortwave radiation and α_{sg}, the ground albedo.

For longwave radiation, the coefficient of reflectivity of the upper layer is $\sigma_f(1 - \epsilon_f)$, of absorptivity $\epsilon_f\sigma_f$ and of transmissivity $(1 - \sigma_f)$, where ϵ_f is the canopy emissivity, and for the ground, ϵ_g.

For longwave radiation budget, we obtain at ground level,

$$R_{Lg} = (1 - \sigma_f)\frac{\epsilon_g(R^{\downarrow} - \sigma T_g^4)}{1 - \sigma_f(1 - \epsilon_f)(1 - \epsilon_g)} - \frac{\epsilon_g\epsilon_f\sigma_f\sigma(T_g^4 - T_f^4)}{1 - \sigma_f(1 - \epsilon_f)(1 - \epsilon_g)} \quad (3)$$

for the canopy,

$$R_{Lf} = \sigma_f\left[\epsilon_f(R^{\downarrow} - \sigma T_f^4) + \frac{\epsilon_f\epsilon_g\sigma(T_g^4 - T_f^4)}{1 - \sigma_f(1 - \epsilon_f)(1 - \epsilon_g)}\right] + \sigma_f\frac{(1 - \sigma_f)(1 - \epsilon_g)\epsilon_f(R^{\downarrow} - \sigma T_f^4)}{1 - \sigma_f(1 - \epsilon_g)(1 - \epsilon_f)} \quad (4)$$

where, T_g and T_f are the ground and canopy temperatures, σ the Stefan-Boltzmann constant and $R^{\downarrow}$ the atmospheric longwave radiation, which is computed from a standard formula (Monteith, 1973), using air temperature T_a and humidity q_a at a given height in the surface layer (here 10 m).

As a first approximation, σ_f constitutes the fractional areal cover of vegetation. Kanemasu (1977), considering various agricultural plants, established a simple relationship between the parameter σ_f and the leaf area index (LAI) as $\sigma_f = 1 - \exp(-\text{LAI} \times 0.4)$.

In the present study, the experimental sites are over the Beauce Plateau, which is covered mainly by wheat. From agronomical studies (Perrier et al., 1978), the LAI is typically constant (around 1 to 2) during tillering. It increases (from 2 to a maximum near 6 to 8) during growth and heading, and decreases to about 3 during maturation. Thus, considering a region covered by a wheat canopy, the LAI ranges from 2 to 6, involving a σ_f from 0.65 to 0.95. In this analysis, LAI is always greater than 3 (from mid-April until harvest); hence σ_f is greater than 0.7 and the soil contribution is always minor in this analysis.

The IR surface temperature, T_s, observed by satellite is clearly different from the canopy temperature T_f and the soil temperature T_g. T_s is determined by the longwave IR radiation available above the canopy surface:

$$\sigma T_s^4 = R^{\downarrow} - R_{Lf} - R_{Lg}. \quad (5)$$

2) PARTITION OF FLUX

As for the radiation balance, following Thom (1972) or Shuttleworth (1977), the canopy may be considered as a single layer, at some height Z_{af} above ground, with both canopy and ground acting as source/sink for momentum, sensible and latent heat. The partition of flux between the ground and the canopy is parameterized as a function of the canopy characteristics, using a conductance formalism.

For momentum transfer, one may write:

$$\tau_f = -\rho C_{fm}U_{af} \quad (6)$$

$$\tau_g = -\rho C_{gm}U_{af} \quad (7)$$

$$\tau = \tau_g + \tau_f = -\rho C_M(U_a - U_{af}) = -\rho U_*^2 \quad (8)$$

where τ, τ_f, τ_g are, respectively, the momentum fluxes above the canopy, to the canopy and to the ground; U_* is the friction velocity and may be estimated from the surface layer wind U_a (at 10 m), using Monin-Obukhov similarity theory, with the stability corrections as given by Louis (1979); (roughness length and displacement height are expressed as a function of LAI and canopy height).

The partition of momentum between τ_f and τ_g is a function of a partition factor σ_α which may be expressed as a function of LAI:

$$\tau_f = \sigma_\alpha\tau \quad (9)$$

$$\tau_g = (1 - \sigma_\alpha)\tau \quad (10)$$

$$\sigma_\alpha = 1 - \frac{0.5}{0.5 + \text{LAI}}\exp(-\text{LAI}^2/8) \quad (11)$$

where (11) was derived by fitting data obtained by Shaw and Pereira (1981), in a model of transfer of momentum within a canopy.

In (6)–(8), U_{af} is the wind speed at canopy level, which both ventilates the canopy and promotes fluxes

from or to the ground. From Thom (1972) it is the hypothetical uniform wind speed which gives the same integrated drag within the canopy as the actual wind profile. The transfer coefficients, C_{fm} and C_{gm}, are relative to exchanges between the canopy (the ground) and the air at the canopy level, and C_M is the aerodynamical conductance in the free atmosphere between the canopy level Z_{af} and the surface layer Z_a. Here C_{fm} controls the momentum exchange between the canopy and the surrounding air. It is generally supposed to be proportional to the leaf area index, and can be written

$$C_{fm} = C_0 U_{af}^{x} \cdot \mathrm{LAI}. \tag{12}$$

Various values for C_0 and x can be found in the literature (see Brutsaert, 1979; Paltridge, 1970; Deardorff, 1977; Thom, 1972), as the exact relationship is likely to be a function of complex canopy parameters, such as leaf shape and orientation, and overall canopy structure. Actually, the exact choice of the formulation in (12) is not very critical in the model. Here we choose Thom (1972) formulation

$$C_{fm} = \frac{U_{af}}{g} \frac{\beta \cdot \mathrm{LAI}}{P_s} \tag{13}$$

where P_s is an empirical shelter factor for momentum transfer, expressed as $P_s = \mathrm{LAI}/2 + 1$, and β allows for the participation of nonfoliage element ($\beta = 1.1$). The wind U_{af} in this formula is in m s^{-1}, as for C_{fm}. So, U_{af} may be solved from (6), (9) and (13), vegetation characteristics and atmospheric data being known. Then, C_{gm} is obtained through (7) and (10), and C_M through Eq. (8).

The same formalism is used for sensible heat transfer, written as

$$H_f = \rho C_p C_{fh}(T_f - T_{af}) \tag{14}$$

$$H_g = \rho C_p C_{gh}(T_g - T_{af}) \tag{15}$$

$$H = H_f + H_g = \rho C_p C_H(T_{af} - T_a) \tag{16}$$

where H, H_f and H_g are, respectively, the sensible heat fluxes above the canopy, to or from the canopy, and to or from the ground; C_p is the specific heat at constant pressure for dry air; C_{fh}, C_{gh} and C_H are conductances equivalent to C_{fm}, C_{gm} and C_M, but for sensible heat transfers. Though Thom showed that the level of exchange could be different for momentum and heat fluxes, we consider that the same level applies for all fluxes. Then C_H for sensible heat transfer may be obtained from the value of C_M for momentum, and C_{gh} from C_{gm}, using aerodynamical transfer relationships and stability corrections between sensible heat and momentum conductances (Louis, 1979). The C_{fh} is modeled like C_{fm} as a function of U_{af} and LAI, but with a different C_0, following Thom (1972), who pointed out that in a canopy the transfer of heat or water vapor encounters a greater aerodynamical resistance than for the transfer of momentum.

Then,

$$C_{fh} = \frac{1}{28} U_{af} \frac{\beta \cdot \mathrm{LAI}}{P_s}, \tag{17}$$

where U_{af} and C_{fh} are also given in m s^{-1}. Latent heat transfer is written in the same way, but one has to account for canopy or soil resistance to evaporation; that is,

$$\mathrm{LE}_f = \rho \frac{C_p}{\gamma} R' C_{fh}[q_{\mathrm{sat}}(T_f) - q_{af}] \tag{18}$$

$$\mathrm{LE}_g = \rho \frac{C_p}{\gamma} \alpha C_{gh}[q_{\mathrm{sat}}(T_g) - q_{af}] \tag{19}$$

$$\mathrm{LE} = \rho \frac{C_p}{\gamma} C_H(q_{af} - q_a) = \mathrm{LE}_f + \mathrm{LE}_g \tag{20}$$

where γ is the psychrometric constant, q_a and q_{af} the partial water vapor pressure, respectively at the surface layer and at the canopy level.

A resistance formalism is used to link the water vapor transfer to the gradient between air water vapor partial pressure and saturation partial pressure at the canopy or the ground surface. Aerodynamic resistances C_{fh}, C_{gh} and C_H are the same as for sensible heat transfers.

3) Canopy and soil resistances

In Eq. (19), α corresponds to the resistance to the diffusion of water through the upper layer of soil when it is not at saturation. Though α is often expressed as a linear function of the ratio of surface soil moisture to some saturation value, we prefer to use a somewhat different concept, letting $\alpha = 1$ when potential evaporation, expressed as

$$\mathrm{LE}_p = \frac{\rho C_p}{\gamma} C_{gh}(q_{\mathrm{sat}}(T_g) - q_{af}), \tag{21}$$

is lower than a limiting evaporation $\mathrm{LE}_{\mathrm{lim}}(w_g)$, where w_g is the surface soil moisture. Alternately, $\alpha = \mathrm{LE}_{\mathrm{lim}}/\mathrm{LE}_p$, when the potential evaporation is larger than that limit. This concept of limiting evaporation is based on the consideration that, for a given soil moisture at a depth d_1 (here taken arbitrarily as 10 cm) in the surface soil layer, which is represented by w_g, the moisture profile above that depth will adapt to the evaporative demand. Owing to the relationship between soil water conductivity and soil moisture, the largest gradient between depth d_1 and the surface (assumed to be completely dry) cannot set up a flux larger than E_{lim}, a function of w_g. For any evaporative demand smaller than E_{lim}, the soil moisture profile will be able to adapt to that demand. The function $E_{\mathrm{lim}}(w_g)$ may be estimated from soil water characteristic functions. As in the present application, the soil contribution to

evapotranspiration is always small, and a rigorous estimation of $E_{\text{lim}}(w_g)$ is not essential.

The R' factor in Eq. (18) accounts for resistance to evaporation, due either to stomatal resistance or to the fact that only a fraction of the total canopy area is contributing to the exchange.

Following Deardorff (1978), R' may be written:

$R' = 1$ for condensation

$$R' = \left(\frac{\text{dew}}{d_m}\right)^{2/3} + \left[1 - \left(\frac{\text{dew}}{d_m}\right)^{2/3}\right] \frac{1}{(\beta + C_{fh}\,\text{RST})}. \tag{22}$$

Thus the model can be used to account for transpiration and for evaporation of free water at the surface of the leaves, where "dew" is the amount of free water on the canopy, and d_m its maximum value; RST is the stomatal resistance. Thus, $R' = 1$ for an entirely wet canopy (dew = d_m) and

$$R'C_{fh} = \frac{1}{\beta/C_{fh} + \text{RST}} \tag{23}$$

for a dry canopy, transpiring only through the leaves, with a stomatal resistance RST.

This factor RST constitutes the essential element of the vegetation parameterization. It basically expresses the efficiency of the foliage transpiration, and as, in this study, the vegetation cover is important (LAI > 2), the energy partition of energy between sensible heat and latent heat is essentially adjusted by the magnitude of RST. In the sensitivity tests, this parameter is allowed to vary over the range of values, likely to be experienced over a wheat canopy (the main crop of the Beauce Plateau). Therefore, the RST variations are accounted for by a representative formulation of RST, based upon agronomical studies (Perrier, 1977; Perrier et al., 1978; Katerji and Perrier, 1983; and others mentioned in Deardorff 1978).

Many physiological and climatological factors are involved in the foliage resistance to evapotranspiration. Among the primary ones, four seem to be most important: the daylight variation, the evaporative demand, the water supply in root zone and the physiological age of the crop. Their parameterization for different cultures is still an open subject of investigation.

Here, we use the formulation proposed by Deardorff (1978), which integrates four factors controlling the evaporative demand

$$\text{RST} = \text{RO}\left[\frac{800}{1 + S^{\downarrow}} + \left(\frac{1.2w_{\text{wilt}}}{0.9w_2 + 0.1w_g}\right)^2\right] \frac{P_s}{\text{LAI}} \tag{24}$$

where $S^{\downarrow}$ is the incident solar flux, w_{wilt} the wilting point for moisture, w_2 and w_g the soil moisture value in the root zone (1 m) and in the surface layer (first 10 cm). The RO includes the seasonal dependence on the physiology of the crop; P_s is the shelter factor, as given before.

To specify the term RO over wheat, we use experimental measurements of wheat stomatal resistance (Perrier et al., 1978) made over two consecutive years, and simultaneously with the evolution of the water supply in the root zone. As shown in Fig. 2, the mean crop resistance RST above wheat, taken at 1300 local time when solar dependence is weaker, is similar for the two years (1975, 1976), from tillering to heading (April to the end of May), around a low constant value (40 to 80 s m^{-1}). However, during the maturation (mid-June to July), the resistances increase abruptly to a higher plateau, from about 60 s m^{-1} to 160 s m^{-1} in 1975 and from approximately 80 s m^{-1} to 340 s m^{-1} in 1976. This large increase corresponds to the phenological aging and drying of the wheat, occurring during this period and involving a reduced crop transpiration. The transition between the two phenological states (growing and maturing) occurs quickly in about two weeks. Higher values of RST in 1976 are evidently related to the water stress of the crop, owing to a large water deficit in soil occurring during the European drought that year.

A simple parameterization of the rapid evolution of RST between the two states (growth and maturing) is for RO to be represented as a step function: a low constant value ($\sim$80 s m^{-1}) during the growth period (mid-April to mid-June) and a high one ($\sim$150 s m^{-1}) during maturation (mid-June to mid-July).

Figure 2 presents the computation of RST, using (24) and employing the specified step function for RO and the experimental measurements of soil water content made by Katerji (1978) and the usual values of foliage density (LAI). There is an acceptable agreement between the calculated and measured values of RST for the two years, considering the relatively rough parameterization of the function influencing RST.

With these derived values of RO, we will use this RST formulation in the sensitivity tests to simulate and study the impact of the RST magnitude on the surface temperature and fluxes and the influence of the water supply upon them for different phenological states.

4) ENERGY BALANCE

Given the flux partition expressed previously, the energy balance equations are solved at both canopy level and ground level.

At canopy level, assuming that thermal inertia within the canopy is negligible, one can write

$$R_{sf} + R_{Lf} = H_f + \text{LE}_f. \tag{25}$$

At ground level, the ground flux is estimated using the force–restore formulation of Blackadar (1976).

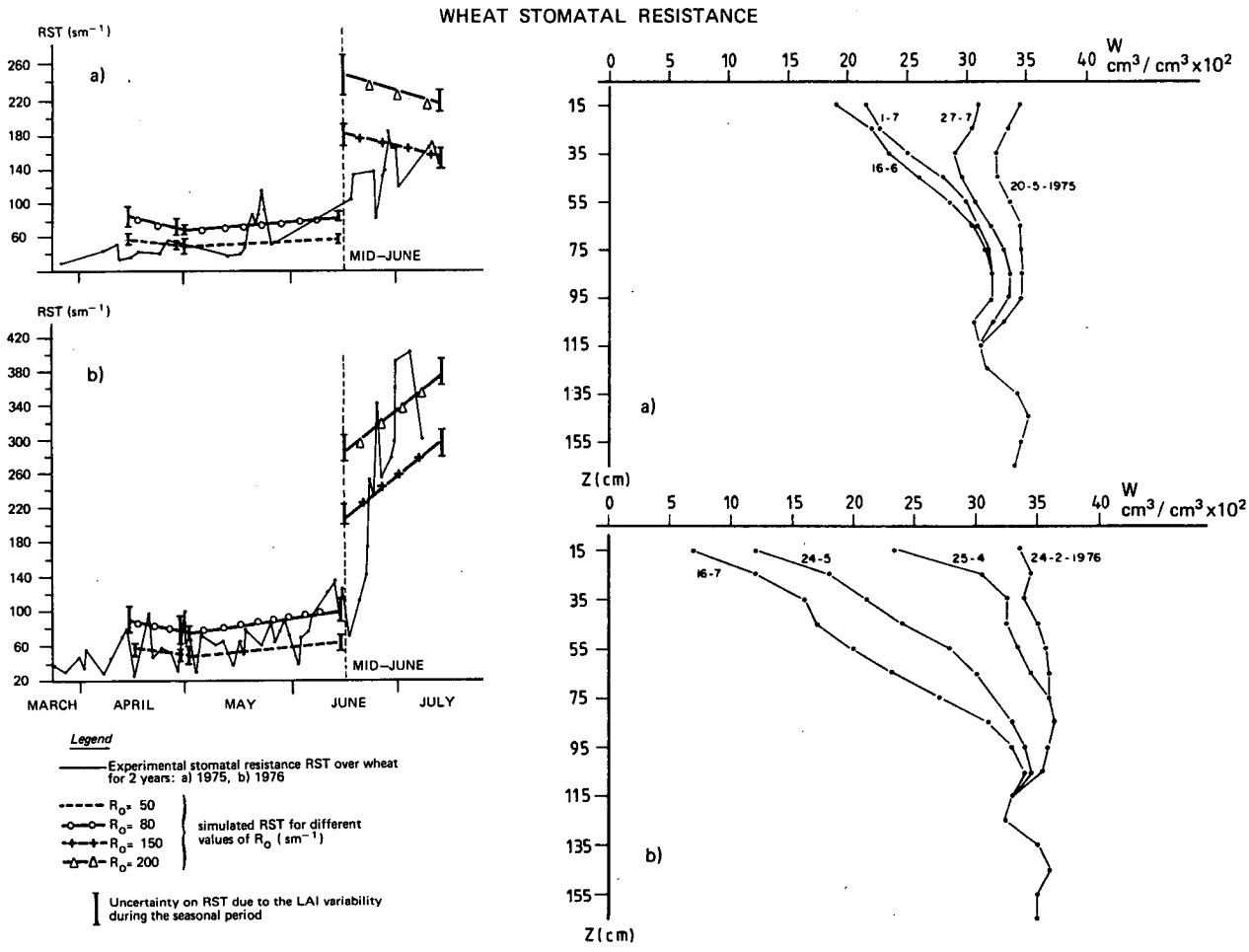

FIG. 2. Seasonal evolution of the stomatal resistance RST above wheat and the soil water content w during two years, (a) 1975 and (b) 1976, from Katerji (1978) data. Comparison with the simulated values of RST (Eq. 24) using the experimental data of w, LAI for different values of RO.

$$G = \frac{1}{C_1}\frac{\partial T_g}{\partial t} + \frac{C_2}{C_1}(T_g - T_2)$$
$$= R_{sg} + R_{Lg} - H_g - \mathrm{LE}_g. \qquad (26)$$

Using relations (1), (2), (3), (4), (16), (20), (25) and (26), the time dependent system is linearized and solved for T_f and T_g, and subsequently the various fluxes. The upper boundary conditions are the atmospheric parameters U_a, T_a and q_a (at 10 m), output of the PBL model, which is, in turn, controlled by the fluxes of the surface model.

3. Sensitivity tests

Our approach now is to consider the main terrain parameters in the interface model as described and to indicate their relative importance. The purpose is to determine what single governing parameter of the group may be inferred by inversion of the model from the use of the midday satellite surface temperature and for what kind of canopy. The nighttime temperatures yield no further significant information about the covering vegetation layer.

Although Deardorff (1978) has proposed a simple and efficient parameterization of a living material, such as a canopy, the list of all parameters describing the interface soil/vegetation in section 2 is, nevertheless, long. To simplify the problem of defining soil/vegetation parameters we propose to study, as a first step, the case of dense vegetation (LAI $\geqslant 2$, $\sigma_f \geqslant 0.65$), suitable for consideration of nearly all of the wheat physiological cycle over the Beauce Plateau (where the LAI is greater than 2 after the wheat rises in mid-April).

As the substrate energy transfers are not of great importance under vegetation canopies with LAI $\geqslant 2$, it is not necessary to test the sensitivity and impact of soil parameters for soil heat and water fluxes. For this reason, the parameterized dependence of soil thermal and water conductivities upon w_g and w_2 is that of

standard clay soils, predominant in the Beauce (see Table 1). Diffusion of water at the soil surface is regulated using the concept of limited evaporation (Eq. 19), where E_{lim} is expressed as an empirical function of w_g,

$$E_{lim}(w_g) = 8.00 \exp(44.0 w_g^2) \frac{0.38}{0.38 - w_g} \quad (27)$$

for w_g in cm^3 cm^{-3} and E_{lim} in W m^{-2}.

Such a relationship indeed depends on the soil characteristics, since it expresses the maximum flux that the surface layer (here 10 cm) can accommodate when average soil moisture in that layer is w_g and the steepest gradient is achieved. However, as in the present application, the soil contribution to evapotranspiration is always small, a rigorous estimation of $E_{lim}(w_g)$ is not essential. Therefore the soil properties appear to depend upon the two soil moistures w_g (the first 10 cm) and w_2 (the first meter). Under a covering canopy, the wheat extracts water quite uniformly in the root zone (around the first meter of soil). Thus, the humidity gradient between w_g and w_2 is lessened, and the assumption of a homogeneous water profile in the first meter of soil (with $w_g = w_2$ and now called w) is regarded as a reasonable simplification for soil characteristics below the canopy.

The number of vegetation parameters are reduced to three essential ones: height h, density LAI and plant resistance for transpiration RST. From experimental agronomical studies above wheat (Perrier et al., 1978; Bonhomme et al., 1978) summarized in Fig. 3, we obtain a typical range of LAI and h which is presented in Table 2. We neglect the variations of canopy height (0.5 m to 1 m from mid-April to July), which has no major influence on the tests. Albedos over countryside areas usually vary in a limited range between 0.15 and 0.25, but surface temperatures and fluxes appear relatively insensitive to surface albedos, as shown by Carlson and Boland (1978). Therefore, the foliage albedo formula with solar inclination is the same for all sensitivity tests and the diurnal range of albedos is between 0.12 and 0.20. To explore in a systematic fashion

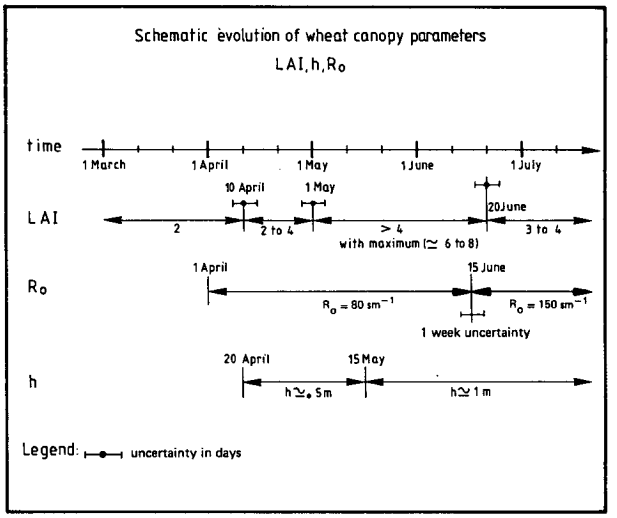

FIG. 3. Seasonal evolution of three parameters (leaf area index, phenological factor RO, height) of the wheat canopy.

the model response to changes in the foliage resistance RST, the different and increasing values of RST used in the tests are calculated from Eq. (24), depending upon the phenological state RO and the soil available water in the root zone. Hence, the remaining soil/vegetation parameters allowed to vary are w, LAI and RST which is a function of RO and w.

For the sensitivity tests, we analyze two days, corresponding to the two phenological states of wheat (growing and mature) 11 May 1982 and 11 July 1982. The two days were clear with strong insolation. The meteorological conditions are given in Table 3.

We consider first the results of the sensitivity tests for the 11 July 1982 for mature crop conditions. The LAI is varied from 2 to a maximum of 8. The value of w, which is used to fix the resistance of the foliage and the resistance of the soil through the concept of limited evaporation, varies between 0.12 cm^3 cm^{-3} (near wilting point) and 0.30 cm^3 cm^{-3} (near saturation). Thus, the variations of RST are calculated from w variations, fixing RO at 150 s m^{-1} for a mature crop.

We examine now the response of the radiative temperature above the canopy [see Eq. (5)], computed by the model at the time of the satellite observation near

TABLE 1. Soil parameters.

Type	Present value
$(\rho C)g$ Specific heat (cal cm^{-3} K^{-1})	$0.26 + w$ (w in cm^3 cm^{-3})
λ_g Thermal conductivity (cal cm^{-1} s^{-1} K^{-1})	$0.0005 + 0.0035\sqrt{w}$
D Hydraulic diffusivity (m^2 s^{-1})	$1.5 \times 10^{-7} \exp[11.2(w - w_s)]$ $w_s = 0.35$ cm^3 cm^{-3} $w_r = 0.15$ cm^3 cm^{-3} w_s saturation soil water content w_r residual soil water content w soil water content

TABLE 2. Model input for sensitivity tests.

	During Seasonal Evolution		
Range for LAI, h, RO	15 April to 15 May RO = 80 sm^{-1} h = 0.5 m LAI 2 to 4	15 May to 15 June RO = 80 sm^{-1} h = 1 m LAI 4	15 June to 15 July RO = 150 sm^{-1} h = 1 m LAI 3 to 4
Range for soil humidity in first meter (volumetric)	w = from 0.30 cm^3 cm^{-3} to 0.12 cm^3 cm^{-3} with w_{sat} = 0.35 cm^3 cm^{-3} w_{wilt} = 0.15 cm^3 cm^{-3}		

TABLE 3. Parameters used in three model simulations.

	11 May 1982	11 July 1982	11 July 1983
Solar radiation at 1200 local time, (W m^{-2})	900	830	800
Hydric deficit of air: $T_a - T_r$ at 2 m at 0600 local time (°C)	0.5	2	−0.1
Relative humidity at 0600 local time (%)	95	88	100
Horizontal wind at 10 m at 1200 local time (m s^{-1})	6.5	6.0	3.2

midday, called T_{sm}, as a function of w and LAI in Figs. 4 and 5. One aspect of these tests stands out. It appears clearly that T_{sm} is less sensitive to the moisture availability in plant and soil than the bare soil temperature. Carlson and Boland (1978) found that the daytime surface temperatures (near 1400 UT) display a full range of about 15°C between extremely dry and moist soils. From our tests (see Fig. 4), the corresponding range is between 5° and 10°C. Thus, the figure leads us to conclude that the surface behavior of bare soil and canopy is different. The uncertainty in the measured surface temperatures by satellite due to uncertainties in the water vapor correction (~1°–1.5°C) is of greater importance over agricultural areas where diurnal variations are considerably less than that over bare soils.

Another important result, obtained from Figs. 4 and 5, is the separation of T_{sm} behavior into two classes: the first one concerns the dense foliage with LAI ≥ 4, where T_{sm} is no longer sensitive to the increasing values of LAI (from 4 to 8); the second class regroups the partial vegetation covering (2 ≤ LAI ≤ 4), where LAI and w are both important.

Since the conclusions concerning two classes are different, we will examine them separately.

a. Results of sensitivity tests over dense canopies (LAI ≥ 4)

The main characteristic is that the response of T_{sm} to changes in LAI and w for RO = 150 s m^{-1} on 11 July 1982, is no longer sensitive to the variations of LAI (tested here from 4 to 8). Thus, for the vegetation, among the three governing parameters (h, LAI, RST), the single remaining one is the mean stomatal resistance RST, for which, as the seasonal factor RO is taken constant, w is used to adjust the magnitude. On the other hand, w also controls the soil regulation α to water diffusion.

But, as expected for a dense canopy, the relative contribution of soil to the total evaporation remains small (between 0 and 20%), even if the water content at the soil surface is important ($w \geq 0.20$ cm^3 cm^{-3}) (Fig. 6). This is due to the small amount of net radiation available at the ground surface (≤150 W m^{-2}), because

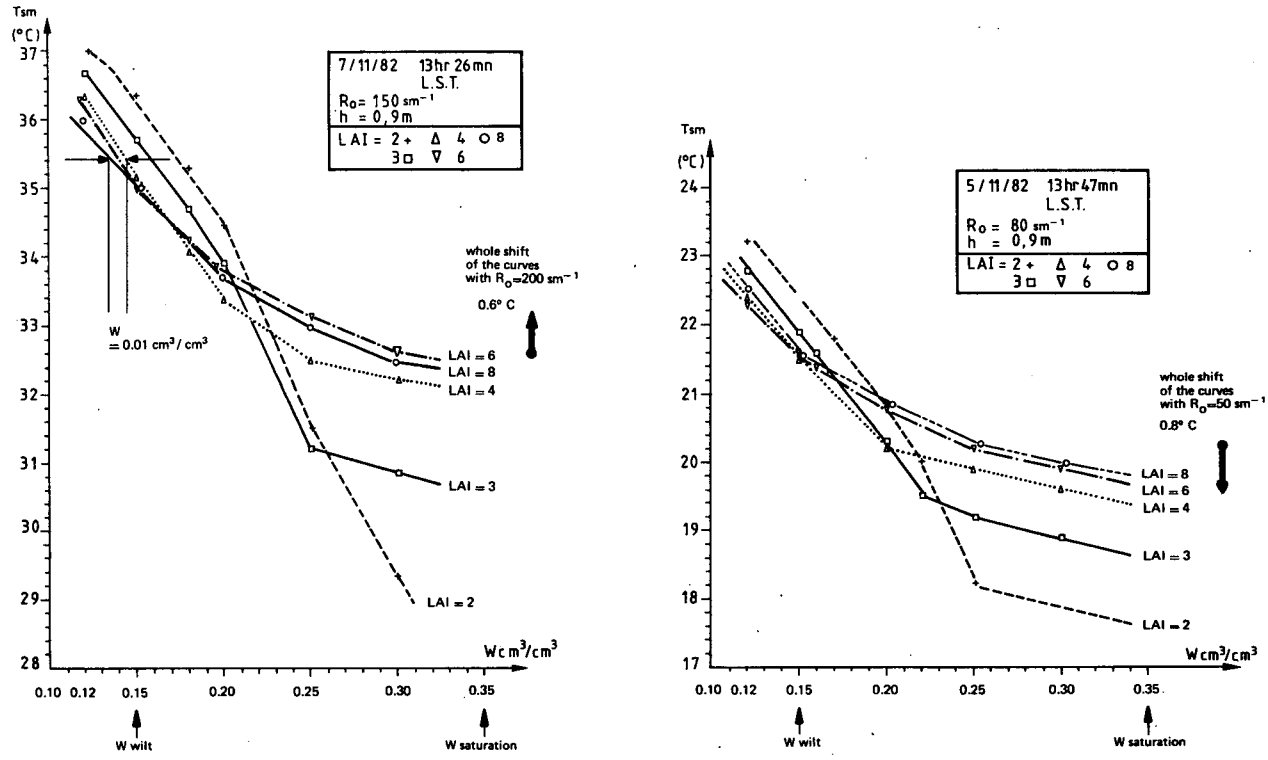

FIG. 4. Variations of the IR surface temperature T_{sm} near midday as a function of the soil humidity content w for given leaf area index (LAI).

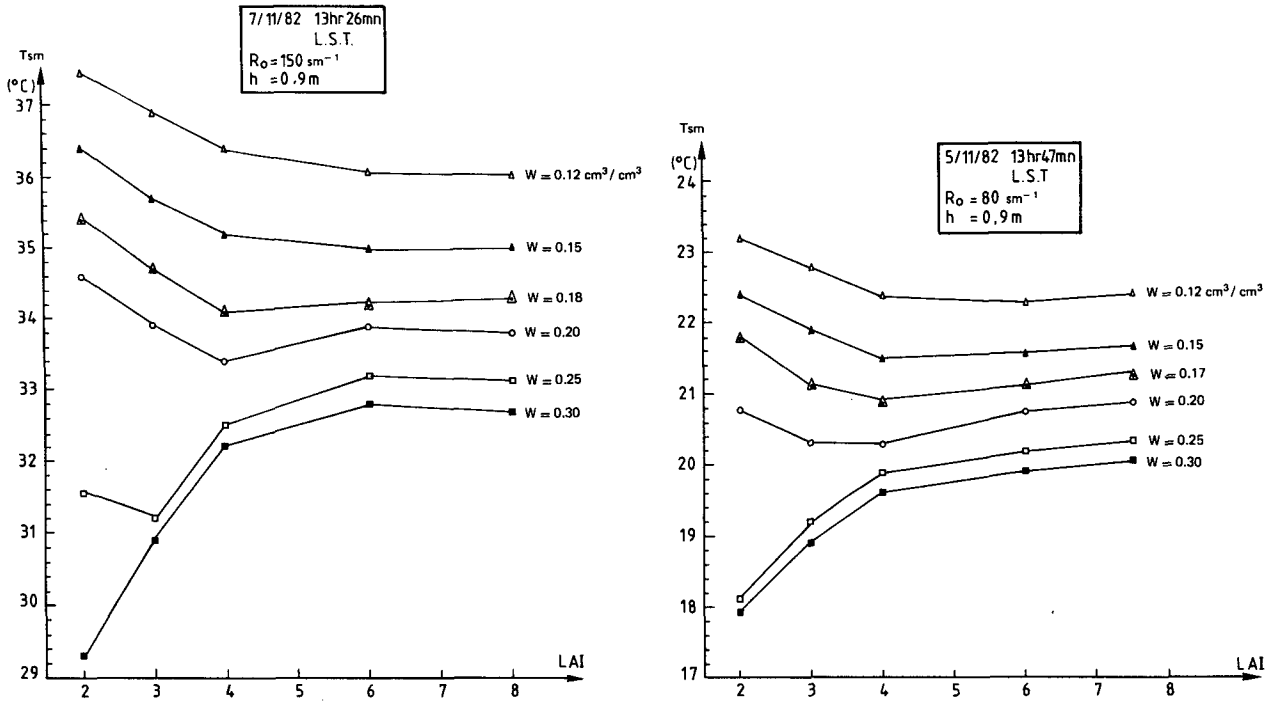

FIG. 5. Variations of the surface temperature T_{sm} near midday as a function of LAI for given soil water content w.

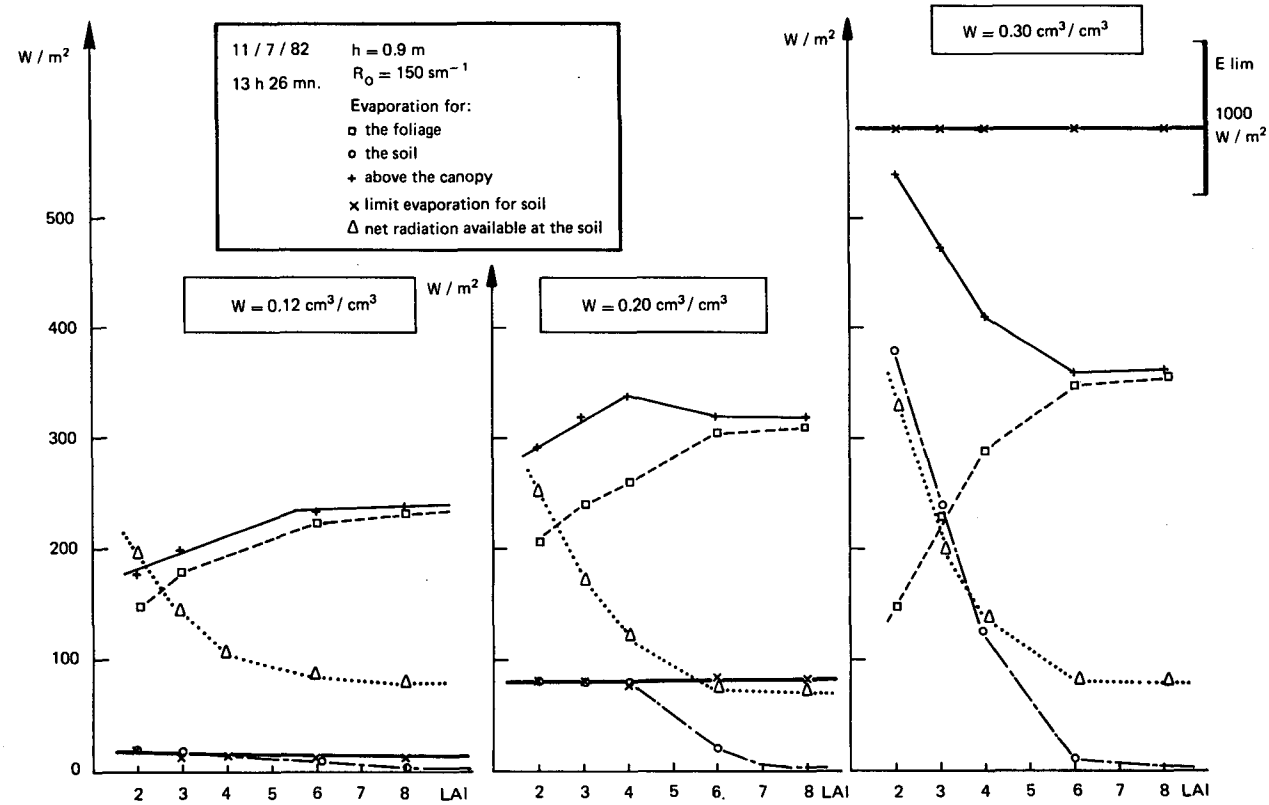

FIG. 6. Relative contribution of soil and foliage to the total evaporation above canopy for the whole range of LAI (2–8) and for three values of soil moisture (w = 0.12; 0.20; 0.30 cm³ cm⁻³).

the foliage density (LAI $\geq$ 4) prevents shortwave radiation from reaching the ground (see Fig. 6). Therefore, the soil parameters are relatively without influence. There remains only one significant parameter to regulate the radiative temperature T_{sm} and the fluxes, namely, the global foliage resistance RST, which is a very different concept from the surface moisture availability used for bare soil, since the vegetation is a layer of negligible heat capacity [see Eq. (25)]. This conclusion can be seen in Fig. 7, where the radiative temperature taken at the time of the satellite observation near midday T_{sm} is clearly a unique function of RST, for the same time (and named RST_m), when its solar dependence is also a minimum. Indeed, these results correspond to agronomical analyses, where, for well-developed vegetation, the foliage density loses its significance and where its evaporation depends on other factors influencing its stomatal resistance.

In consideration of Figs. 4 and 7, the impact of foliage resistance RST_m, over dense canopies, may be separated into two regimes. First, for a relatively weak water supply in root zone (w between 0.12 and 0.22 $cm^3\ cm^{-3}$, approximately half of the total range of w), the w variations induce large variations of T_{sm} ($\sim$3°C, from Fig. 4) and RST_m (from 200 to 400 s m^{-1} in Fig. 7), compared with the rest of the range of w (between 0.22 and 0.30 $cm^3\ cm^{-3}$). In that range, T_{sm} variations are only of 1°C and RST_m varies from 100 to 200 s m^{-1}. Therefore, for w between 0.12 to 0.22 $cm^3\ cm^{-3}$, taking from the model simulations the unique relation between the radiative temperature and the foliage resistance at the time of the midday satellite observation, as in Fig. 7, we can use the measurement of the radiative temperature by the satellite near midday to obtain, with reasonable accuracy, the single factor RST_m of the canopy, without a knowledge of LAI. We estimate the uncertainty to be about $\pm$20 s m^{-1} (Fig. 7), in the range of tested w and for LAI between 4 and 8.

The RST_m is the direct variable inferred by model inversion given the measured radiative surface temperature at midday. An indirect measure of the water content w in root zone may be deduced from RST by a significant parameterization of RST upon w. With regard to the formulation for RST [Eq. (24)], we can estimate that, with no information on LAI, the uncertainty on w calculated from T_{sm} (see Fig. 4) is about

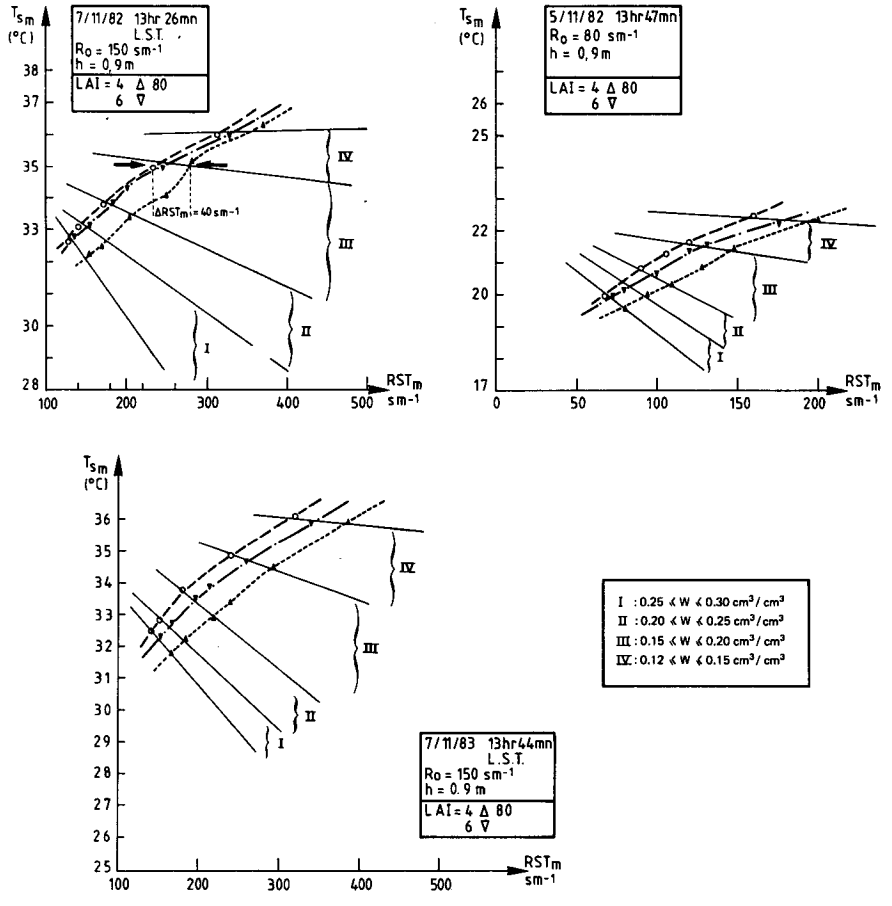

FIG. 7. As in Fig. 5 but as a function of the foliage resistance RST_m (near midday), for dense canopies (LAI $\geq$ 4).

0.01 cm^3 cm^{-3}. However, we must emphasize that the real uncertainty in the soil moisture estimation by this kind of method, is likely much greater than 0.01 cm^3 cm^{-3}. If we exclude for the moment the external sources of errors which may affect the accuracy of the T_{sm} measurements and so w (as the atmospheric correction, the model boundary conditions), the main source of error is the present difficulty in establishing a correct empirical parameterization of RST as a function of the different physiological and meteorological factors (see Katerji and Perrier et al., 1983).

For example, in the formulation used for RST [Eq. (24)], the RO step function (RO = 80 s m^{-1} during growth and 150 s m^{-1} during maturation) is derived from comparison with the data of Fig. 2, and the uncertainty of the two values of RO is about 30 to 50 s m^{-1}. The RO is between 50 and 80 s m^{-1} for growth and between 150 and 200 s m^{-1} for maturation. If we use the value of 200 s m^{-1} for RO in the previous sensitivity tests, rather than 150 s m^{-1}, we obtain a whole shift of the T_{sm} curves (as function of w and LAI) of about 0.6°C. In the range of w from 0.12 to 0.22 cm^3 cm^{-3}, the uncertainty of RO (using 150 s m^{-1} or 200 s m^{-1}) implies an uncertainty on w estimation of about ±0.015 cm^3 cm^{-3}, which is reasonable. However, the determination of the empirical function of RST calls for further research. Thus, we cannot really quantify the uncertainty of w from the measurement of RST_m. Hence, the absolute soil moisture estimation inferred by this method for studying the temporal evolution of w on a given area, from multitemporal satellite thermal images, requires complementary information on RST. But, the methodology can still be used for determination of spatial variability of soil moisture at a regional scale.

Examination of the response of evaporation at midday, LE_m, to the changes of LAI, RO, and w, the analysis and conclusions are very similar to those for T_{sm} for dense foliage (LAI ≥ 4) (Fig. 8). The evaluation of the maximum evaporation flux, at the satellite orbit time, LE_m, is possible, given a measurement of the radiative temperature T_{sm}, without having to specify LAI (Fig. 9). The uncertainty on LE_m is small, about 20 W m^{-2}, for an LAI between 4 and 8, and for all the range of dry and moist soils. As the variations of LE_m are regular with T_{sm}, for all the range of dry and moist soils under canopies, a given uncertainty in the measurement of T_{sm} leads to the same uncertainty in LE_m, for low and high evaporation rates.

We now have to consider the second regime, corresponding to a good water supply in the root zone (w between 0.22 to 0.30 cm^3 cm^{-3}). Variations of w induce weak variations of RST_m (from 120 to 200 s m^{-1}) and reduced sensitivity of T_{sm} (~1.5°C), from Figs. 4 and 7. However, it appears that for moist soil conditions ($w \geq 0.22$ cm^3 cm^{-3}), T_{sm} and LE_m reach a plateau and become more or less insensitive to w (see Figs. 4 and 8). This plateau expresses the maximum foliage evapotranspiration reached by a well-developed vegetation, with an adequate water supply, where the soil

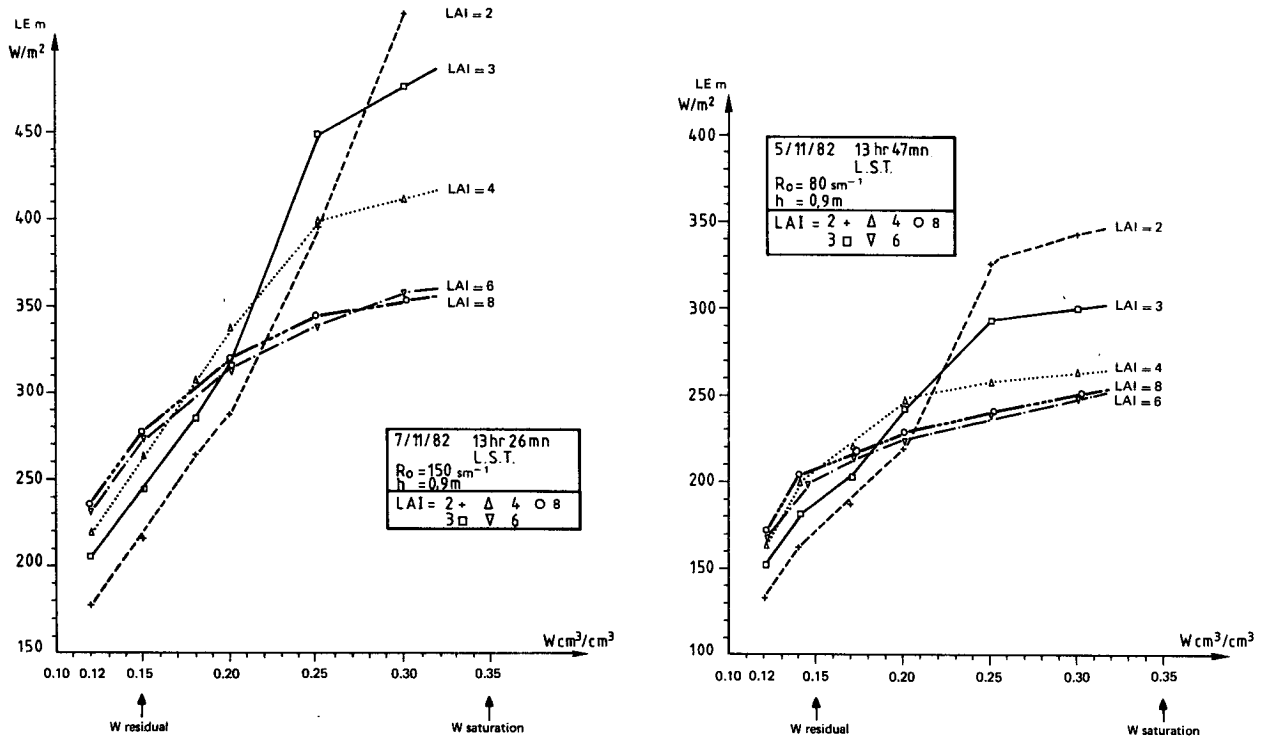

FIG. 8. Variations of evapotranspiration LE_m near midday as a function of soil humidity content w for given LAI.

water is no longer a limited factor for the root absorption. We may remark that, for a large water supply, the foliage resistance RST_m reaches effectively a minimum (here between 120 to 200 s m^{-1}) for a given phenological state (mature, for the 11 July 1982). Even at a minimum value, the foliage resistance RST by the formulation (24) never reaches a zero resistance, leading to potential evaporation. The equation expresses the fact that, wide open leaf stomata do not possess a zero resistance, as is the case with saturated bare soil. Thus, the maximum value of canopy evaporation can never reach the potential evaporation (Perrier, 1977).

For that range of w between 0.22 and 0.30 cm^3 cm^{-3}, the uncertainty of RST_m from the measurement of T_{sm} is also about ± 20 s m^{-1} (see Fig. 7). For determining w from the value of T_{sm}, with the formulation used for RST [Eq. (24)], the uncertainty in w has increased, as the temperature T_{sm} reaches a limiting minimum value. The uncertainty of w is about ± 0.03 cm^3 cm^{-3} (see Fig. 4). With RO varying from 150 to 200 s m^{-1} the uncertainty of w becomes very large (around ± 0.04, ± 0.05 cm^3 cm^{-3}). Hence, for that range of w, even if the computation of RST is accurate, we have no precise estimation of w.

The same conclusions, as given for dense canopies, remain valid for the second day of simulation (11 May 1982) for the growing state of wheat (RO = 80 s m^{-1}). The ranges of uncertainty on RST_m in w are the same for the two regimes considered.

b. *Results of sensitivity tests for partial canopy cover ($2 \leqslant LAI \leqslant 4$)*

For partial canopy cover, with LAI between 2 and 4, LAI is no longer a negligible factor, especially for relatively moist soils (w between 0.20 and 0.30 cm^3 cm^{-3}) (see Fig. 5). For that range of w, the contribution of the soil evaporation is comparable with the foliage transpiration, or even greater (see Fig. 6). As an example, for a water content near saturation (w = 0.30 cm^3 cm^{-3}), soil evaporation exceeds the foliage evaporation for LAI $\leqslant$ 3 (Fig. 6), increasing significantly the total surface latent flux and decreasing the radiative surface temperature. Over bare soil and near saturation, the soil resistance becomes nearly zero and leads to a potential evaporation, unlike the case for vegetation where the potential rate is never achieved, as explained in section 3a.

Therefore, for a partial canopy, we find it necessary to describe precisely both water transfer by the foliage (including its foliage density LAI and stomatal resistance RST) and the water diffusion at the soil surface depending on the soil resistance α which is a function of soil humidity w_g near the surface. The assumption of a constant water profile from the soil surface to 1 meter in soil (with $w_g = w_2 = w$) is no longer valid. Identical results have been found from experimental studies on growing lucern (Katerji and Perrier, 1985).

In the case of partial foliage cover, the only use of midday radiative temperature T_{sm} is not sufficient to infer the several governing parameters (LAI, RST, α). Although estimates of LAI may be obtainable from the visible channels of meteorological satellite (the AVHRR of NOAA, or the MSS of LANDSAT), it is not possible to specify the humidity in the first few cm of soil (and thus α) by remote sensing at the scale of a satellite pixel. The number of surface parameters to infer are hence too numerous actually for satellite methodologies.

Meanwhile, we may remark that, for relatively dry soils (0.12 cm^3 $cm^{-3} \leqslant w \leqslant$ 0.20 cm^3 cm^{-3}) and with the assumption of no soil water gradient ($w_g = w_2 = w$), T_{sm} is not very sensitive to LAI (Fig. 4). The value of w (and so of RST_m and α) is deduced from T_{sm}, without a knowledge of LAI, with a reasonable accuracy of ± 0.015 cm^3 cm^{-3} (Fig. 4). Thus, in the case of dry soils, the soil evaporation remains weak compared to the foliage evapotranspiration (Fig. 6).

c. *Sources of experimental uncertainties*

The maximum variation in T_{sm} for LAI $\geqslant 4$ is likely to be 4–5°C. This means that for relatively dry soils (w between 0.12 and 0.22 cm^3 cm^{-3}), an accuracy of ± 0.5°C in T_{sm} corresponds to an error of about ± 0.02 cm^3 cm^{-3} in w (see Fig. 4). The absolute value of T_{sm} simulated by the model depends on the specified boundary layer and initial conditions, especially the accuracy in the temperature profile, for example, as might be obtained from a sounding at 0600 UT. These errors are not likely to exceed about ± 0.5°C on the average, corresponding to an uncertainty of ± 0.3°C in T_{sm}, which is reasonable considering the typical T_{sm} range (4° to 5°C) over canopies with or without water stress. The uncertainty involved in the mean canopy resistance RST_m is about ± 40 s m^{-1}, with the same value for dry and wet soils, and the uncertainty on LE_m is about ± 20 W m^{-2} for low and high evaporation rates (see Figs. 7 and 9). For relatively dry soils (w between 0.12 to 0.22 cm^3 cm^{-3}), where T_{sm} is the more sensitive to w, the inaccuracy of ± 0.3°C on T_{sm} leads therefore to a reasonable uncertainty of ± 0.01 cm^3 cm^{-3} on w (see Fig. 4).

In general, these errors are smaller than those originating from uncertainties in the measured IR surface temperatures, arising largely from the atmosphere water vapor correction. Therefore, when measured IR satellite temperatures are used to obtain the soil moisture by inversion of the model, such measurement uncertainties (which are likely to approach or exceed ± 1°C) provide a possibly greater source of error in obtaining w than does the model itself.

4. Test region and satellite image processing

a. *The test region: la Beauce*

The test region is located southwest of Paris and is delimited on the map of Fig. 10 by the square, 128 km

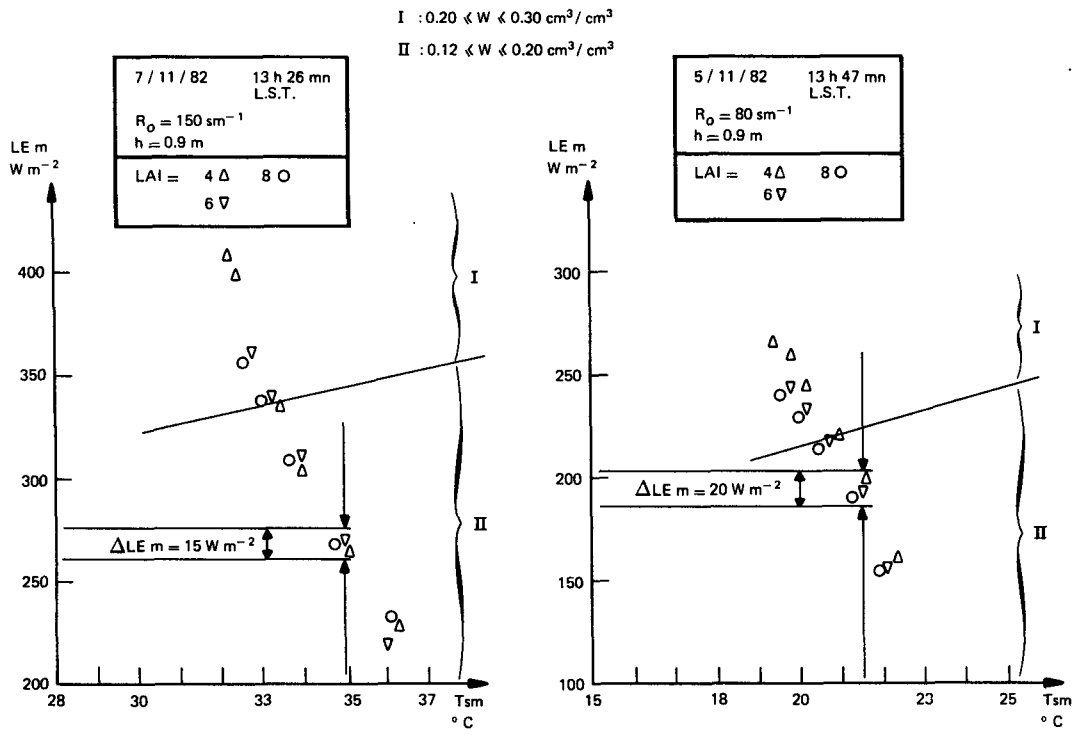

FIG. 9. As in Fig. 8 but as a function of the radiative surface temperature T_{sm}. (Uncertainty on the evaluation of LE_m from T_{sm}.)

on a side. The Beauce Plateau is situated at the center. It is composed of two different areas: the Grande Beauce at the east around the town of Pithiviers and the Beauce Chartraine at the west around the city of Chartres (see Fig. 10). The relief appears to be quite flat increasing from 130 m MSL in the east to 170 m MSL in the west. At the west end of the Beauce Plateau are the Faux Perche and the first hills of the Perche. The two regions are quite different from the Beauce Plateau by relief, geology and crop cover distribution.

Over the two areas of the Beauce Plateau, (Beauce Chartraine and Grande Beauce) the pedological covering (approximately the first meter of soil), corresponding to the root zone for vegetation, is very similar, namely limon. But below, the geological substratum of the plateau itself is divided into two regions which correspond approximately to the natural areas described before. The east is formed by Aquitanien limestone while the west consists of Senonien white chalk with silex. This structure induces differences in the draining properties of the two regions. Table 4 gives the crop cover distribution for the year 1979–80 in the Grande Beauce and the Beauce Chartraine. The Plateau has a homogeneous cover of vegetation, mainly wheat and barley (50%) and corn (20%), if one excludes sugar beet which is not present in the Beauce Chartraine. The crop distribution is homogeneous inside each region.

b. Satellite image processing

To obtain surface thermal structure at a regional scale, the Advanced Very High Resolution Radiometer of the NOAA satellites is convenient. This satellite is able to scan a given location four times a day (at intervals of 6 h) at a time very close to local maximum temperature (approximately 1400 UT). This heliosynchronous polar satellite allows data acquisition with a resolution of 1.1 km at zero scan angle and a sensitivity of 0.1°K. The image processing involves calibration, registration and correction for water vapor absorption. The radiometric calibration is done using the coefficients given by the AVHRR on-board calibration. Temperature analyses for different daytime images were rectified to geographic coordinates. Registration and resampling finally lead to an image with one-kilometer square pixels and a geographic error less than 3 or 4 km (for more details, see Cheevasuvit et al., 1985). A spatially constant water vapor correction is applied using the Lotran 4 model (Deschamps and Phulpin, 1980). Atmospheric moisture data were obtained from radiosonde or airplane information over Beauce.

As recalled in Section 2, using a picture segmentation procedure on the IR NOAA images at midday, the spatial variability of temperature over the Beauce Plateau has a very defined signature (see Cheevasuvit et al., 1985). The region is divided in three or more large

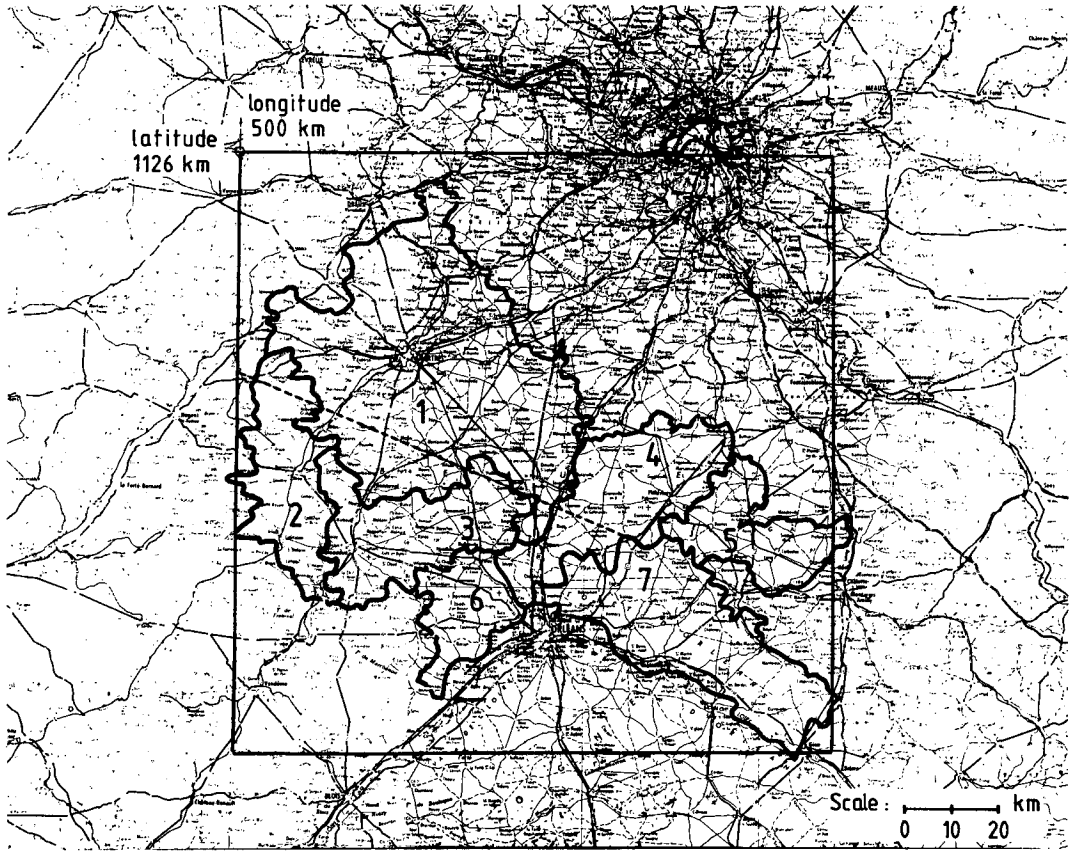

FIG. 10. The two different areas of Beauce Plateau are west, Beauce Chartraine (1) extended by Beauce Dunoise (3), and east, Grande Beauce (4) extended by Beauce de Patay (6). Outside Beauce Plateau is Faux Perche (2) (west).

areas (greater than 20 × 20 km) of distinct mean surface temperature, but where the inner variability of temperature is very weak (about 1°–2°C). Hence, the surface parameters defined by the model are representative of the scale of these homogeneous subzones. The segmentation processing is applied to the 3 midday NOAA images studied: 11 May and 11 July 1982 and 11 July 1983. In Fig. 11, the segmentation results on the three images are presented. The images are classified in quasi-homogeneous subzones of temperatures, with an inner variability given by the threshold ϵ of the image. The difference between the maximum and minimum of temperatures in each zone is defined as $\leqslant\epsilon$. Hence, the homogeneous subzones, greater than 20 km × 20 km are individualized on the Beauce Plateau for the three images and their mean surface temperatures T_{sm} then estimated (see Fig. 11).

TABLE 4. Crop distribution in the natural regions (%).

Region	Wheat	Barley	Corn	Sugar beet
Grande Beauce	40	20	10	20
Beauce Chartraine	50	10	25	1

* Source: Agriculture general census 1979–80.

An interesting feature of the 11 May and 11 July 1982 cases is that Beauce Chartraine is clearly colder than the Grande Beauce for the two different seasons. Table 4 indicates that the difference is not likely due to differences in vegetation cover. As an approximation, we assume that the phenological state of wheat over the two regions of Beauce are the same. Applying the results of the sensitivity tests on T_{sm} (see section 3), we note that the temperature gradient between the two regions may be related to a difference of foliage resistance RST_m, if the canopies are dense. We shall quantify the RST_m difference between the Grande Beauce and the Beauce Chartraine, and the induced water content difference in the next section.

A validation is proposed by comparison between the simulated surface fluxes and the experimental measurements at two sites, located in the two different homogeneous subzones. The experimental fluxes are calculated by methods which integrate the turbulent scale of a few kilometers. They are thus comparable with the scale of several AVHRR pixels. That comparison is a partial validation of the proper choice of the model parameterizations, by showing that the model, using T_{sm} data, simulates the correct surface fluxes, by an adequate estimation of the foliage resistance RST_m.

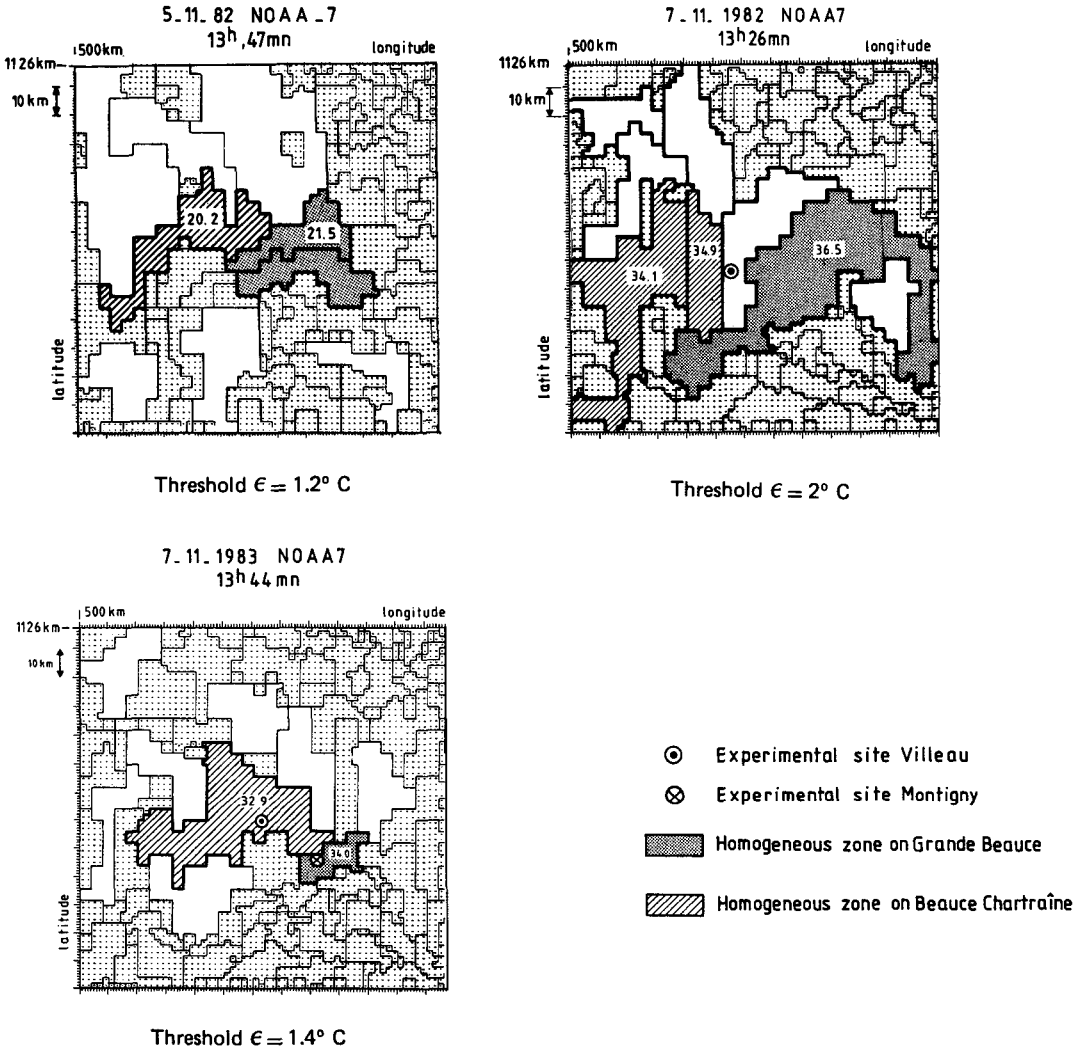

FIG. 11. Results of the segmentation on the three studied images. The greatest homogeneous areas (≥400 km²) are underlined. Zones (cross hatching/stippling) are homogeneous areas in Beauce Chartraine or Grande Beauce. Corrected temperatures (in °C) are specified.

We also apply the methodology to the 11 July 1983 image, where, with a rainy beginning to the month, there is no clear difference of surface temperature between Grande Beauce and Beauce Chartraine.

5. Case studies

For the three cases, 11 May 1982, 11 July 1982, and 11 July 1983, we study the determination of the important soil/vegetation parameters which must be adjusted in the model, in order that the measured satellite surface temperatures near midday by NOAA-7 (Fig. 12) correspond to the model temperatures at the same time. The surface fluxes over the two regions (Beauce Chartraine and Grande Beauce) subsequently can be derived.

Over the Beauce Plateau, the crop is homogeneous, mainly wheat and barley (60% of the total area). For nearly all of the wheat physiological cycle, the foliage density of the canopy remains important (LAI is greater than two following the wheat sprouting in mid-April) (Fig. 3). The results of the sensitivity tests for dense vegetations (section 3) remain appropriate to the analysis of the three cases. We assume, as the crop distribution is quasi-identical in the two regions of the Beauce Plateau, that the LAI is the same over them. For the two 11 July cases in 1982 and 1983, one or two weeks before harvest, the wheat is mature and LAI reaches a plateau of about three to four. Cornfields, a minority crop in these two regions (~20%), have about the same LAI. Therefore, we may estimate the regional LAI at a reasonable value of three to four, at the lower limit of the range of a dense canopy (see section 3a). For the third case, 11 May 1982, the wheat crop is growing and the LAI in May is at a maximum, about five to seven, corresponding surely to a dense canopy.

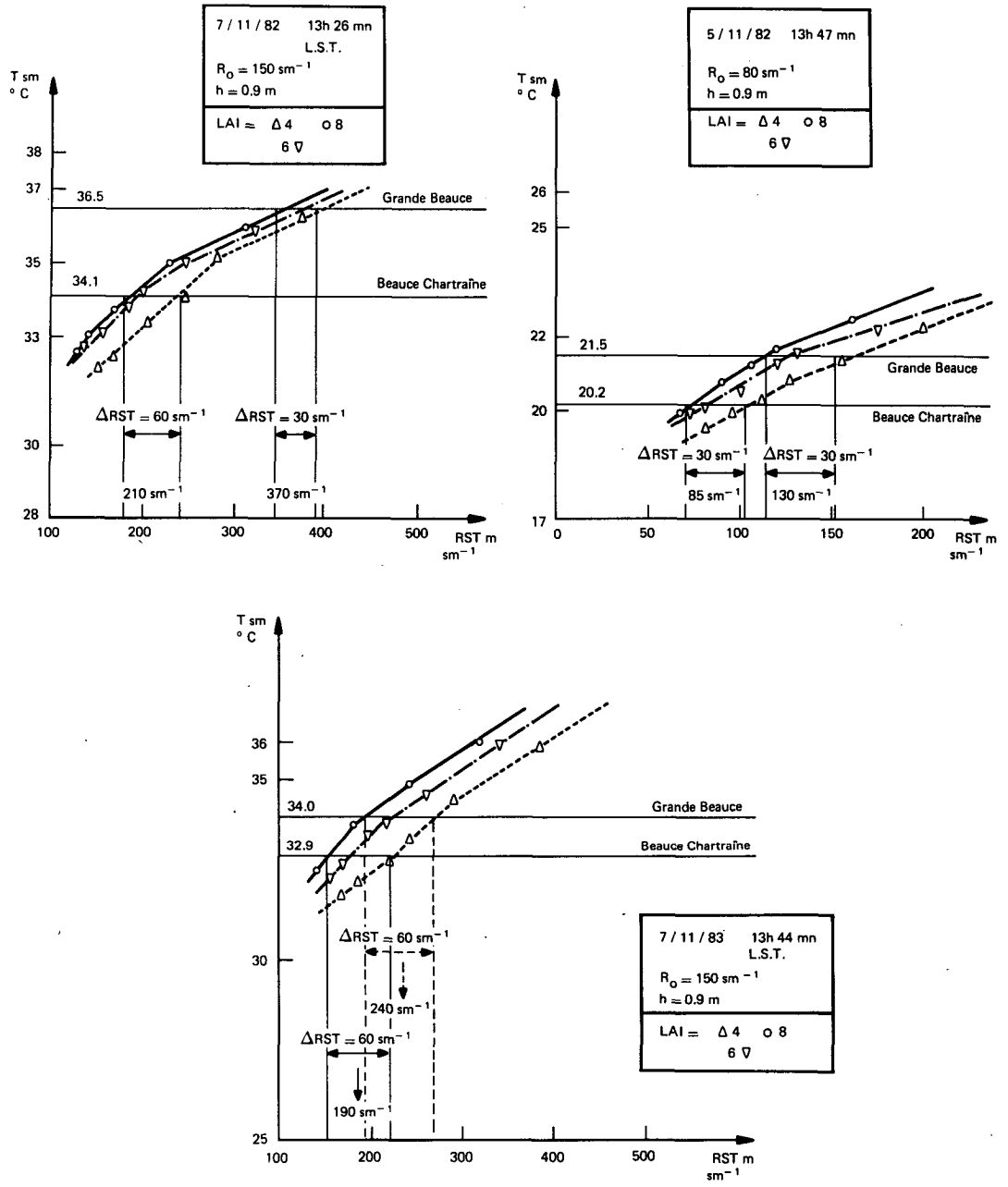

FIG. 12. Determination of the canopy resistance RST_m from sensitivity tests on the three days 11 July 1982, 11 July 1983 and 11 May 1982 for the two regions, Beauce Chartraine and Grande Beauce.

The soil parameters, as thermal and hydraulic conductivities are fixed (see section 3) by parameterizations for standard clay-type soils, dominant in the Beauce Plateau.

As surface temperatures and fluxes appear especially insensitive to surface albedo (Carlson and Boland, 1978), the foliage albedo α_{sf} is taken to be identical for the two regions and the three dates, varying from 0.12 (near midday) to 0.20 (during night) with solar inclination. Effectively, values of about 0.10 to 0.15 have been found over the region with the visible channel of AVHRR, for several days of mid-July 1983 (T. Carlson, personal communication).

Now, we apply the results of the sensitivity tests for dense canopies (LAI $\geq$ 4) as seen in section 3a, for the measured radiative temperatures on the homogeneous segmented areas of Beauce Chartraine and Grande Beauce (Fig. 11). Therefore, setting the unique relation between the radiative temperature and the foliage resistance at the time of the midday satellite observation,

TABLE 5. Simulated canopy and soil parameters on 11 July 1982 and 1983 and 11 May 1982 on the two regions of Beauce Chartraine and Grande Beauce.

	Common parameters for the two regions		Adjusted parameters				
			Mean foliage resistance RST_m (s m^{-1})			Soil water content w (cm^3 cm^{-3})	
Date	Leaf area index LAI	Height h (m)	Grande Beauce	Beauce Chartraine	RO (s m^{-1})	Grande Beauce	Beauce Chartraine
11 May 1982 13 h 47 min	5–7	0.9	130 ΔRST_m = 30 s m^{-1}	85 ΔRST_m = 30 s m^{-1}	80	0.15 Δw = ±0.01 (due to RO varying from 80 to 50 s m^{-1})	0.20 Δw = ±0.03
11 July 1982 13 h 26 min	3–4	0.9	370 ΔRST_m = 30 s m^{-1}	210 ΔRST_m = 60 s m^{-1}	150	0.12 Δw = ±0.01 (due to RO varying from 150 to 200 s m^{-1})	0.18 Δw = ±0.01
11 July 1983 13 h 44 min	3–4	0.9	190 ΔRST_m = 60 s m^{-1}	240 ΔRST_m = 60 s m^{-1}	150	0.16 Δw = ±0.01 (due to RO varying from 150 to 200 s m^{-1})	0.19 Δw = ±0.02

RST_m and T_{sm}, by model simulations as in Fig. 7, we can use the measurement of the radiative temperature by NOAA-7 near midday to obtain the single important parameter RST_m, the foliage resistance, and then the surface fluxes. The values of RST_m over the Beauce Chartraine and the Grande Beauce are obtained by this method in Fig. 12 and given for each of the three cases in Table 5. The uncertainty in RST_m, due to no accurate specification of LAI, are estimated from Fig. 12. As seen in Section 3a, they vary effectively between ±20 and ±30 s m^{-1}.

The RST_m is the direct variable inferred by model inversion from the measurement of the midday radiative temperature T_{sm}. We now deduce the indirect value of the water content in the root zone, using the proposed formulation of RST [Eq. (24)]. The values of w are calculated from the model simulations of the response of the radiative temperature at the satellite orbit time T_{sm} with w and LAI (⩾4) variations, and using the measurements of T_{sm} by NOAA-7 over the Beauce Plateau (see Fig. 13). The values found are recapitulated in Table 5, with their uncertainties associated with the unspecified LAI and RO (Δw is around ±0.01, ±0.02 cm^3 cm^{-3}). We have for the three cases (except for Beauce Chartraine on 11 July 1983) the favorable case of dense canopies with a relatively dry root zone (w between 0.12 and 0.20 cm^3 cm^{-3}), where we may infer with a minimum of ambiguity the value of w from the measurement of the radiative temperature T_{sm}.

Thus, for the three days we obtain measurements of the mean canopy resistance at a regional scale and in turn, indirect measurements of the water supply w (in the first meter of soil). Despite the simplifications of the boundary layer/vegetation model, and the rough parameterization of RST [Eq. (24)], the relative variations (in time and space) of RST and w, derived for the three cases, appear to be realistic.

One of the ultimate objectives, of course, is to derive the correct partition of the surface fluxes on the scale of the satellite pixel and the test of a good model is whether it can yield a partition of the surface fluxes corresponding with the measurements of these fluxes. Therefore, a comparison has been made between simulated fluxes and experimental measurements of sensible heat flux H and net radiation R_N at two representative sites of the two regions (Villeau for Beauce Chartraine and Montigny for Grande Beauce), for the two 11 July cases.

For July 1982, the surface sensible heat flux was computed from an instrumented 100-m mast at Villeau. For July 1983, the sensible heat flux was measured at the two sites, by the same probes and by two different methods: first, with a local SAMER methodology (Itier, 1981), measuring vertical gradients of temperature and wind in the surface layer, and second, with an acoustic Doppler sounder (Weill et al., 1980) using turbulent parameterization of the well-mixed layer. The acoustic Doppler sounder computes surface heat flux at a representative scale of a few square kilometers, similar to the AVHRR scale (1 km^2 resolution). As the two sites were in homogeneous monocultural areas, we have found that the two methodologies of sensible heat flux measurements at local and mesoscale gave identical experimental data. Hence, in Fig. 15, we mention only the SAMER results for July 1983.

Figures 14 and 15 present the simulated and measured fluxes for July 1982 and July 1983. The sets of

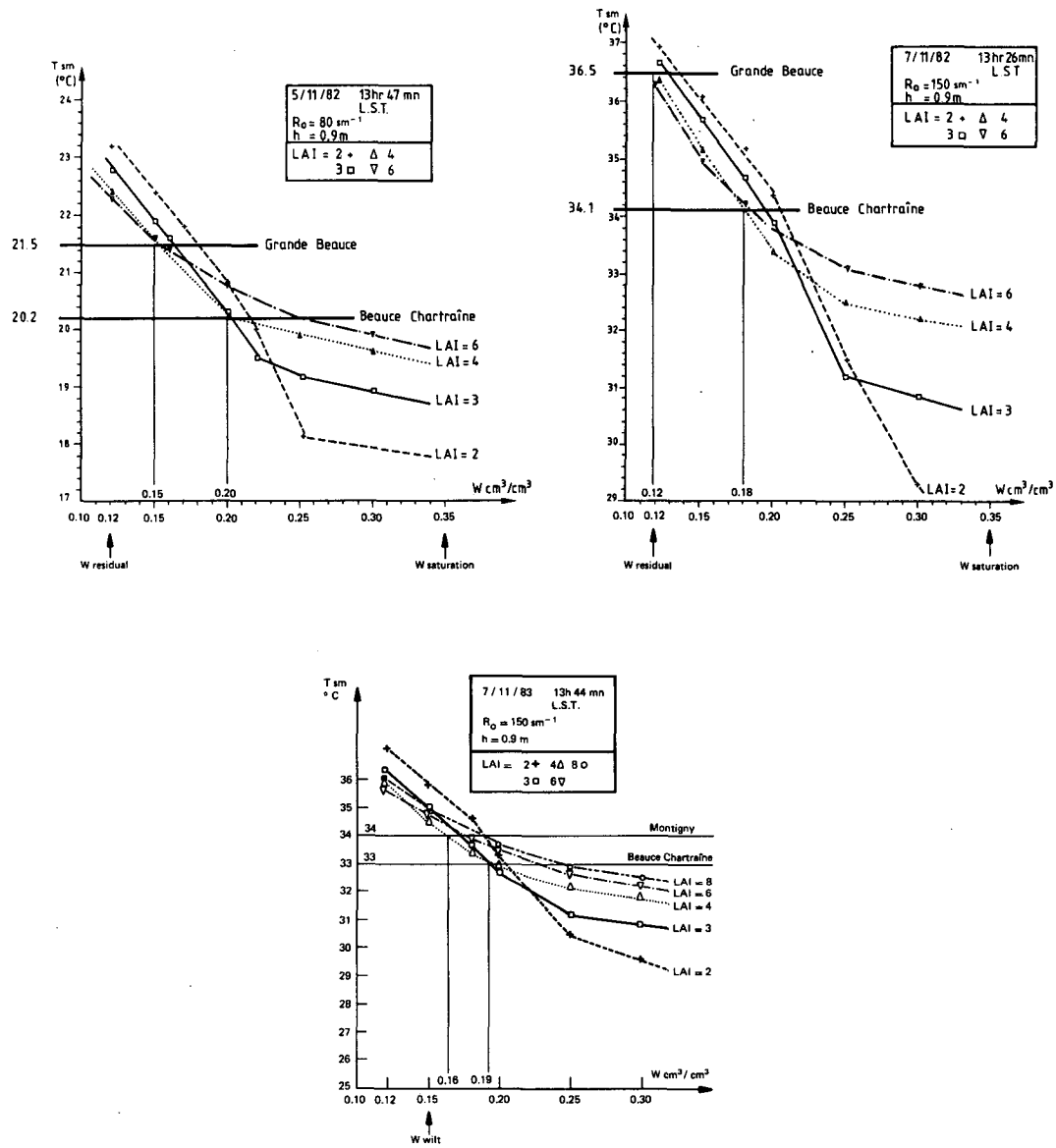

FIG. 13. Determination of the water content w from sensitivity tests on the three days 11 July 1982 and 1983 and 11 May 1982 for the two regions, Beauce Chartraine and Grande Beauce.

variables are those determined from the model sensitivity tests on T_{sm} (Figs. 12 and 13): for July 1982, LAI = 4, RO = 150 s m^{-1}, and w = 0.12 cm^3 cm^{-3} for the Grande Beauce and w = 0.18 cm^3 cm^{-3} for the Beauce Chartraine; for July 1983, the same values of LAI, RO were used and w = 0.16 and 0.19 cm^3 cm^{-3}, respectively, for the Grande Beauce and the Beauce Chartraine. A good comparison of computed sensible heat flux at midday with the measured fluxes is found on the two days. The different climatological conditions between these two years are, reflected by the difference in sensible heat fluxes, 300 W m^{-2} for 11 July 1982 versus 150 W m^{-2} for 11 July 1983. This good comparison between simulated and measured fluxes are an added support to the choice of our canopy resistance parameterization.

This methodology produces also a spatial heterogeneity of surface fluxes between two regions, especially for the 11 July 1982, where the temperature difference between Grande Beauce and Beauce Chartraine is very striking (2.5°C). The spatial estimated gradient is of 80 W m^{-2} (a relative variation of 30%) for sensible heat flux and 100 W m^{-2} (around 60%) for evaporation.

The two images of May and July 1982 exhibit an important thermal contrast between the east and west parts of the Beauce Plateau, the Grande Beauce and the Beauce Chartraine (see Fig. 11). The results of our model simulations have shown that the thermal dif-

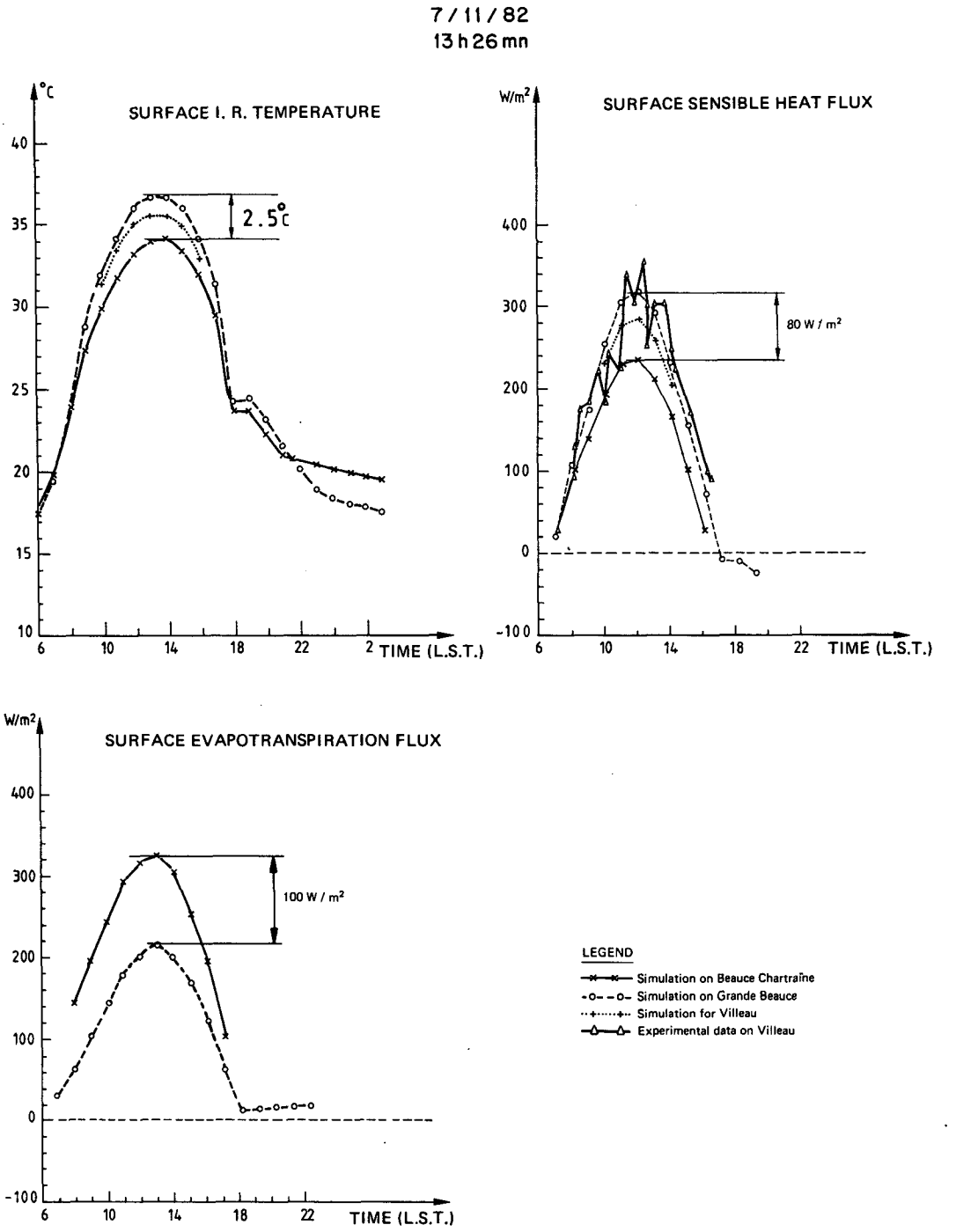

FIG. 14. Experimental and simulated fluxes on the two regions of study (Grande Beauce and Beauce Chartraine) for 11 July 1982. The surface parameters are LAI = 4, RO = 150 s m^{-1}, h = 0.9 m and, respectively, $w = 0.12$ cm^3 cm^{-3}, $w = 0.18$ cm^3 cm^{-3} for Grande Beauce and Beauce Chartraine. Symbols are the same for all the simulations.

ference is explained by a spatial variation of the actual water content under classical vegetation and have quantified that difference. Grande Beauce appears to be drier than Beauce Chartraine, especially on 11 July 1982, with a 30% difference of w (w is 0.12 cm^3 cm^{-3} on the Grande Beauce and 0.18 cm^3 cm^{-3} on the Beauce Chartraine).

Nevertheless, the water content in the root zone on a regional scale or on the scale of a AVHRR pixel has no definition in the present state of the art. As a con-

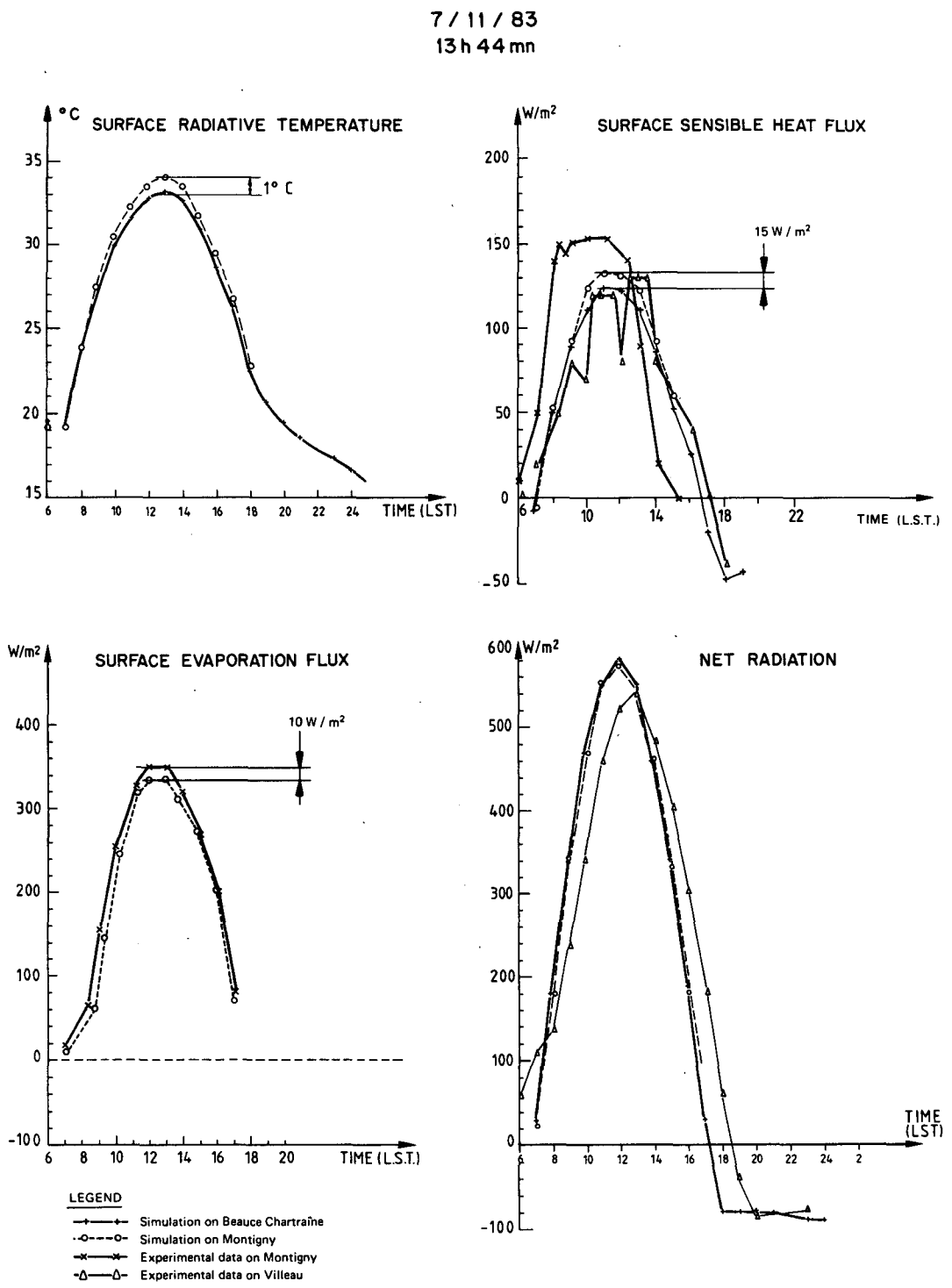

FIG. 15. Experimental and simulated fluxes on the two subject regions for 11 July 1983. The surface parameters are LAI = 4, RO = 150 s m^{-1}, h = 0.9 m and, respectively, w = 0.16 cm^3 cm^{-3}, w = 0.19 cm^3 cm^{-3} for Grande Beauce and Beauce Chartraine.

sequence, it is difficult to compare the product of our methodology to any ground-truth measurements. But, a document exists for the Beauce Plateau (Lafrechoux and Studer) which gives the regional distribution, not of the actual water content at the same dates, but of a soil property, "the soil available water," associated with

the soil water drainage in the surface (1st or 2nd meter of soil), and confirms the existence of a gradient of soil humidity between Grande Beauce and Beauce Chartraine.

This soil property, the "soil available water" is defined as the quantity of water (expressed as height of water), which can be stored between the field capacity and the wilting point in the entire root zone ($w_{\text{field capacity}} - w_{\text{wilt}}$). The results are based on pedological and geological data over the region and have been verified using 183 sampled profiles. In Fig. 16, the "soil available water" map is represented at the same scale as the segmented 11 July 1982 image of AVHRR. The homogeneous segmented areas over Beauce Chartraine and Grande Beauce determined from the AVHRR IR image are clearly correlated, together with the borders of the areas, with two regions of greater and less "soil available water" respectively (see Fig. 16). This can be understood by the fact that since Grande Beauce has a weaker total water supply in the soil surface, the water content in the root zone is more quickly exhausted at the end of the wheat culture in July, than in Beauce Chartraine. This leads to an area of smaller water content for Grande Beauce in July 1982. This feature was enhanced in 1982, a particularly dry year over the Beauce according to climatological analyses of the *Météorologie Nationale* over 30 years. The year 1983 is clearly moister.

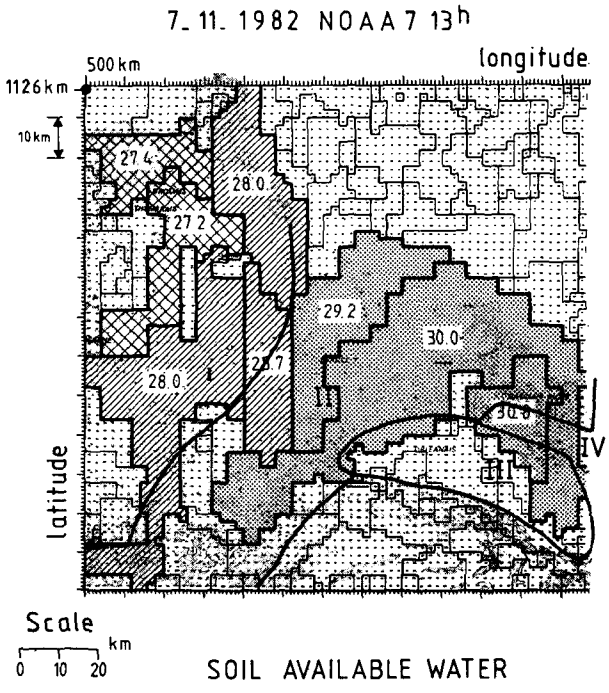

FIG. 16. Comparison between the homogeneous areas of July 1982 and regions of equal soil water availability. There is a very good agreement between the two maps. The thermal structure may be used as an indicator of the soil water budget. (I) 150 to 200 mm available water with dry valleys (75 to 100 mm); (II) 100 to 150 mm with dry valleys (25 to 50 mm); (III) 50 to 75 mm; (IV) 75 to 100 mm.

Moreover, we find in July 1983, at the same time of year, that the two regions of Grande Beauce and Beauce Chartraine are quite thermally identical, with a midday temperature of 32.9°C, leading to a measurement of $w = 0.19$ cm^3 cm^{-3} from our model simulations (see Fig. 13). This value of w for the Grande Beauce is clearly greater than in the 11 July 1982 case ($w = 0.12$ cm^3 cm^{-3}).

The good behavior of the water content evolution w over Grande Beauce for these two climatologically different years support the choices of the parameterizations and simplifications of our methodology for studying an agriculturally homogeneous region.

6. Conclusions

In this paper, we present a method and its limits for the evaluation of evaporation over a rural canopy at a regional scale, from measurements of the infrared surface temperatures by satellite. The model is based on the application of a one-dimensional atmosphere/vegetation model. The noticeable feature of the model is that it accounts for the foliage canopy, assuming an adequate partition of the available energy fluxes between ground and vegetation by introducing a representative canopy resistance to water vapor diffusion, following Deardorff (1978).

To simplify the problem of the numerous soil/vegetation parameters involved in the Deardorff formulation, we have restricted our study to the case of dense vegetation, where the number of parameters may be reduced to four primary ones: height, foliage density and resistance for vegetation, and mean water content in the root zone for soil. With the aid of sensitivity tests on these parameters, we have shown that, over dense homogeneous cultures (LAI $\geqslant 4$), the midday satellite temperature can be used to obtain, by model inversion, the only remaining influential parameter, the canopy resistance RST, and hence the correct surface fluxes. The canopy resistance RST constitutes a very different approach from the concept of moisture availability used for bare soils, as the vegetation is a layer of negligible heat capacity. From sensitivity tests, we estimate the uncertainty of RST to be about ± 20 s m^{-1}.

From the expression of the canopy resistance, one can obtain the substrate water content in the root zone, using a relationship to RST proposed by Deardorff (1978), but modified using measurements made over wheat during two years (Perrier et al., 1978). Accordingly, w is estimated with an uncertainty of about ± 0.01 cm^3 cm^{-3} for relatively dry soils (w from 0.12 to 0.20 cm^3 cm^{-3}) and about ± 0.03 cm^3 cm^{-3} for moist soil (0.20 to 0.30 cm^3 cm^{-3}).

It is likely, however, that the real uncertainty on w is much greater than these estimates, due to the lack

of real empirical formulation of RST, as a function of the different physiological and meteorological factors. However, the formulation [Eq. (24)] used in this study is a rather simple one for quantifying results of this methodology. If the absolute value of w is difficult to estimate in practice, this methodology can still be used for determining the spatial variability of soil water on a regional scale.

This methodology has been applied over a flat quasi-monocultural region (the Beauce, covered by wheat), where the analysis of the AVHRR imagery indicates a separation of the Beauce, into two homogeneous temperature zones (20 km × 20 km), each with a different temperature, suggesting that each zone possesses a different substrate water supply. Experimental measurements of the surface fluxes on the Beauce verify the simulated fluxes and thus provide added support for our choice of the canopy resistances. A difference of the draining soil properties between the two zones is also confirmed qualitatively by pedological studies (Lafrechoux and Studer).

However, the absolute determination of soil water content is precariously dependent on a judicious calculation of the canopy resistance. It remains to test further the vegetation resistance formulation under a variety of cultural systems (corn, meadows, etc.) from experimental studies over several years and regions. The ultimate aim would be to understand the relation between the IR surface temperatures and fluxes on a more complex patchwork of cultures.

Acknowledgments. The authors would like to thank their colleagues of the *Météorologie Nationale,* INRA (*Institut National de Recherche Agronomique*) and CRPE who participated in this work. Special thanks are due to B. Itier (INRA) for his SAMER data, to G. Therry (*Météorologie Nationale*) for modeling advice, and G. Rochard (CMS, *Centre de Météorologie Spatiale*) for satellite processing. This project was supported by the CNES (*Centre National d'Etudes Spatiales*). The satellite images have been received at the CMS at Lannion (France). Cordial thanks are also due to T. Carlson (Pennsylvania State University), for the final discussions.

APPENDIX

List of Symbols

c_p	specific heat in general
C_{fm}, C_{gm}, C_M	momentum transfer coefficient: within the canopy, at the soil, in the surface layer at the reference level
C_{fh}, C_{gh}, C_H	heat transfer coefficient: within the canopy, at the soil, and in the surface layer at the reference level
d	displacement height
dew	mass of liquid water on the foliage
d_m	maximum value of dew
H_f, H_g, H	sensible heat flux: within the canopy, above the ground, above the canopy
LAI	leaf area index
LE_f, LE_g, LE,	latent heat flux: within the canopy, above the ground, above the canopy
LE_m	value of LE at the time of the satellite observation near midday.
q	specific humidity
q_{af}	mean specific humidity of air within the canopy
q_a	specific humidity of air at reference level in surface layer
P_s	shelter factor for momentum
R'	fraction of potential evaporation rate from the foliage
$R^{\downarrow}$	atmospheric longwave radiation
R_{sg}, R_{sf}	available visible radiation: at ground level, in the canopy
R_{Lg}, R_{Lf}	available longwave radiation: at ground level, in the canopy
RST	stomatal resistance of foliage
RST_m	value of RST at the time of the satellite observation near midday
RO	seasonal dependence factor of RST
$S^{\downarrow}$	incoming shortwave radiation
T	absolute temperature
T_{af}	mean air temperature within the canopy
T_f	leaf surface temperature
T_g	ground surface temperature
T_s	infrared surface temperature
T_{sm}	value of T_s near midday at the time of the satellite orbit
T_a	temperature of air at reference level in surface layer
U_a	wind at reference level in surface layer
U_{af}	mean wind speed within the canopy
U_*	friction velocity
w	global soil moisture in the root zone (around 1st meter of soil)
w_g	volumetric concentration of soil moisture in the upper 10 cm (d_1)
w_2	soil moisture content within the first meter (d_2)
w_{wilt}	a wilting point value of w
β	constant for participation of nonfoliage elements in momentum conductance
α_{sf}, α_{sg}	albedo: foliage, ground surface
α	fraction of potential evaporation rate from the soil surface
ϵ_f, ϵ_g	emissivity: foliage, ground surface
σ_α	partition factor of momentum flux between vegetation and soil
σ	Stefan-Boltzmann constant
σ_f	average shielding factor defined as the degree to which the foliage prevents shortwave and longwave radiation from reaching the ground

τ_f, τ_g, τ momentum flux: within the canopy, at soil, in the surface layer

ρ density of air

REFERENCES

Becker, F., E. Hechinger and M. Raffy, 1982: Comparison between the accuracies of a new discretization method and an improved Fourier method to evaluate heat transfers between soil and atmosphere. *J. Geophys. Res.*, **87**, 7325–7339.

Blackadar, A. K., 1976: Modeling the nocturnal boundary layer. *Third Symp. Atmospheric Turbulence, Diffusion and Air Quality*, Raleigh, Amer. Meteor. Soc., 46–49.

Bodin, S., 1979: A predictive numerical model of the atmospheric boundary layer based on the turbulent energy equation, SMHI Report 13, Norrköping, Sweden.

Bonhomme, R., J. C. Guinade, G. Guyot and Ph. Malet, 1978: Variation de la structure d'un couvert végétal en fonction de son état pluviologique. Utilisation possible de la télédétection/IUFRO. *Symp. on Remote Sensing*, Freiburg.

Brutsaert, W., 1979: Heat and mass transfer to and from surface with dense vegetation, *Bound.-Layer Meteor.*, **16**, 365–388.

Carlson, T. N., and F. E. Boland, 1978: Analysis of urban-rural canopy using a surface heat flux/temperature model. *J. Appl. Meteor.*, **17**, 998–1013.

——, J. K. Dodd, S. G. Benjamin and J. N. Cooper, 1981: Satellite estimation of the surface energy balance, moisture availability and thermal inertia. *J. Appl. Meteor.*, **20**, 67–87.

Cheevasuvit, F., O. Taconet and D. Vidal-Madjar, 1985: Thermal structure of an agricultural region as seen by NOAA7-AVHRR. *Remote Sensing of Environment*, **17**(2), 153–163.

Deardorff, J. W., 1977: A parameterization of ground surface moisture content for use in atmospheric prediction models, *J. Appl. Meteor.*, **16**, 1182–1185.

——, 1978: Efficient prediction of ground surface temperature and moisture with inclusion of a layer of vegetation. *J. Geophys. Res.*, **83**(4), 1889–1903.

Deschamps, P. Y., and T. Phulpin, 1980: Atmospheric correction of infrared measurements of sea surface temperature using channels at 3.7, 11 and 12 μm. *Bound.-Layer Meteor.*, **18**, 131–143.

Idso, S. B., R. D. Jackson and R. J. Reginato, 1977a: An equation for potential evaporation from soil, water and crop surfaces adaptable to use by remote sensing. *Geophys. Res. Lett.*, **4**, 187–188.

Itier, B., 1981: Une méthode simple pour la mesure de l'évapotranspiration réelle à l'échelle de la parcelle. *Agron. J.*, **1**(10), 869–876.

Kanemasu, E. T., U. D. Rosenthal, R. J. Raney and L. R. Stone, (1977): Evaluation of an evapotranspiration model for corn. *Agron. J.*, **69**, 461–464.

Katerji, N., and A. Perrier, 1983: Modélisation de l'évapotranspiration réelle ETR d'une parcelle de luzerne: rôle d'un coefficient cultural. *Agron. J.*, **3**(6), 513–521.

——, and A. Perrier, 1985: Determination de la résistance globale d'un couvert végétal à la diffusion de vapeur d'eau et de ses différentes composantes; Approche théorique et vérification expérimentales sur une culture de "luzerne", *Agric. Meteor.*, (to be published).

Lafrechoux, M., and R. Studer: Esquisse des caractères techniques des sols de la région Centre. Chambre Régionale d'Agriculture du Centre, Ed.

Louis, J. F., 1979: A parametric model of vertical eddy fluxes in the atmosphere. *Bound.-Layer Meteor.*, **17**, 187–202.

Monteith, J. L. 1973: *Principles of Environmental Physics.* Elsevier, 241 pp.

Paltridge, G. W., 1970: A model of growing pasture, *Agric. Meteor.*, **7**, 93–130.

Perrier, A., 1977: Projet de définitions concernant l'évapotranspiration en fonction de considérations théoriques et pratiques. *La météorologie, Numéro spécial "Evapotranspiration."*

——, N. Katerji, G. Gosse and B. Itier, 1978: Etude "in situ" de l'évapotranspiration réelle d'une culture de blé. *Agric. Meteor.*, **21**, 295–311.

Prevot, L., R. Bernard, O. Taconet and D. Vidal-Madjar, 1984: Evapotranspiration from a bare soil moisture data. *Water Resour. Res.*, **20**(2), 311–316.

Price, J.-C., 1977: Thermal mapping: A new view of the earth. *J. Geophys. Res.*, **82**, 2582–2590.

Seguin, B., S. Baelz, S. M. Monget and V. Petit, 1982: Utilisation de la thermographie I.R. pour l'estimation de l'évaporation régionale. *Agron. J.*, **2**(1), 7–16.

——, and B. Itier, 1983: Using midday surface temperature to estimate daily evaporation from satellite thermal I.R. data. *Int. J. Remote Sens.*, **4**(2), 371–383.

Shaw, R. H., and A. R. Pereira, 1981: Aerodynamic roughness of vegetated surfaces. The effect of canopy structure and density, *15th Conf. of Agriculture and Forest Meteorology and Fifth Conf. on Biometeorology, April 1–3, 1981, Anaheim, Calif.*, Amer. Meteor. Soc.

Shuttleworth, W. J., 1977: Simplified 1-D model of vegetation atmosphere interaction, *Bound.-Layer Meteor.*, **14**, 3.

Therry, G., and P. Lacarrère, 1983: Improving the eddy kinetic energy model for planetary boundary layer description. *Bound.-Layer Meteor.*, **25**, 63–88.

Thom, A. S., 1972: Momentum, mass and heat exchange of vegetation. *Quart. J. Roy. Meteor. Soc.*, **98**, 124–134.

Watson, K., 1975: Geologic applications of thermal infrared imagery. *Proc. IEEE*, **63**, 128–137.

Weill, A., C. Klapisz, B. Strauss, F. Baudin and C. Jaupart, 1980: Measuring heat flux and structure functions of temperature fluctuations with acoustic doppler sodar," *J. Appl.. Meteor.*, **19**, 199–205.

Wetzel, P. J., and D. Atlas, 1983: Inference of soil moisture from geosynchronous satellite infrared observations. *Proc. Sixth Conf. Biometeorology and Aerobiology*, Amer. Meteor. Soc., April 25, 1983.